DEPARTAMENTO DE CIÊNCIAS DA VIDA

FACULDADE DE CIÊNCIAS E TECNOLOGIA
UNIVERSIDADE DE COIMBRA

Characterization of the innate immune response to *Alternaria infectoria*

Mariana Luísa Cruz e Almeida

2013

DEPARTAMENTO DE CIÊNCIAS DA VIDA

FACULDADE DE CIÊNCIAS E TECNOLOGIA
UNIVERSIDADE DE COIMBRA

Characterization of the innate immune response to *Alternaria infectoria*

Dissertação apresentada à Universidade de Coimbra para cumprimento dos requisitos necessários à obtenção do grau de Mestre em Bioquímica, realizada sob a orientação científica da Professora Doutora Teresa Maria Fonseca Oliveira Gonçalves (Universidade de Coimbra)

Mariana Luísa Cruz e Almeida

2013

Acknowledgements

I am extremely grateful to Professor Teresa Gonçalves for her supervision as well as for believing in me.

I would like to acknowledge Professor Olga Borges for her availability.

I would also like to express my gratitude to Professor Paula Veríssimo and Professor Rodrigo Cunha.

Most of all to my family, friends and colleagues, for the patience, support and encouragement.

Index

List of tables

List of figures

List of abbreviations

Ado - adenosine

Adora 2a - A_{2A} adenosine receptor gene

AIDS - acquired immunodeficiency syndrome

AMP - antimicrobial peptides

cAMP - 3'-5'-cyclic adenosine monophosphate

ASC - apoptosis-associated speck-like protein containing a Card

ATP - adenosine 5'-triphosphate

BCL-10 - B cell lymphoma 10

BSA - Bovine serum albumin

Card9 - caspase recruitment domain-containing protein 9

CLR - C-type lectin receptor

CR3 - complement receptor 3

CREB - cAMP response element-binding protein

DAMP - damage-associated molecular patterns

DC - dendritic cell

DC-SIGN - dendritic cell-specific intercellular adhesion molecule-3-grabbing non-integrin

DMEM - Dulbecco's modified Eagle's medium

EPAC - exchange factor activated by cAMP

ERK - extracellular signal-regulated kinase

FcγR - Fc receptor gamma-chain

FBS - fetal bovine serum

HEPES - 4-(2-hydroxyethyl)-1-piperazineethanesulfonic acid

IDO - indoleamine 2,3-dioxygenase

IL - interleukin

IFN - interferon

iNOS - inducible nitric oxide synthase

IRF3 - interferon-regulated factor 3

ITAM - immunoreceptor tyrosine-based activation motif

LPS - lipopolysaccharides

MatI1 - mucosa-associated lymphoid tissue lymphoma translocation protein 1

MOI - multiplicity of infection

MR - mannose receptor

Myd88 - myeloid differentiation primary response protein 88

NADPH - nicotinamide adenine dinucleotide phosphate

NLRP3 - NOD-, LRR- and pyrin domain-containing 3

NF-κB - nuclear factor kappa-light-chain-enhancer of activated B cells

PAMP - pathogen-associated molecular patterns

PBS - phosphate buffered saline

PDA - potato dextrose agar

PLCγ2 - phospholipase C gamma 2

PRR - pattern-recognition receptor

RAF - RAF proto-oncogene serine/threonine-protein kinase

ROI - reactive oxygen intermediates

ROS - reactive oxygen species

Sky - spleen tyrosine kinase

TLR - toll-like receptor

TNF-α - tumor necrosis factor alpha

TMB - tetramethylbenzidine

WGA - wheat germ agglutinin

YME - yeast malt extract

ζP - zeta potential

Abstract

Over the last decades, fungal infections emerged as life-threatening diseases, mainly due to the increase of the immunocompromised population. For this reason, *Alternaria infectoria* comes forth as a rare opportunistic pathogen, which by being one of the most common airborne pathogens, can give rise to numerous manifestations of human disease.

The host immune system is a major determinant of which particular forms of disease will develop after exposure to fungi. Traditionally considered only as the first line of defence, innate immunity has recently received renewed attention because, despite a certain lack of specificity, it effectively distinguishes between self and non-self, eventually leading to the activation of adaptive immune mechanisms by the generation of unique signals.

This work had the main goal of characterizing the innate immune response of macrophages to *A. infectoria*, a rare yet opportunistic human pathogen. Included in this broader objective are the study of *A. infectoria* conidia-macrophage interaction and the role of A_{2A} adenosine receptors in the macrophage response to *A. infectoria* conidia infection.

The most important conclusion drawn is that *A. infectoria* conidia do not trigger a proinflammatory response in macrophages. Firstly, no increase in the production and release of TNF-α was found during *A. infectoria* conidia infection of macrophages. Secondly, the Adora 2a gene expression did not change with the macrophage infection by conidia. Thirdly, extracellular ATP levels did not increase substantially with *A. infectoria* conidia infection. In addition, *A. infectoria* conidia recognition by macrophages proved to be independent from TLR2 signaling, while A_{2A} adenosine receptors were found to accumulate in clusters during conidial infection. Moreover, we conclude that regardless of the engulfment of conidia by macrophages, a very fast process, macrophages neither delayed germination in phagocytosed conidia, nor did they stop mitotic division, even while containing internalized conidia.

The more is discovered about the interactions between fungi and the immune system, the better are the chances of develop more effective antifungal agents.

Keywords: *Alternaria infectoria*, conidia, innate immune response, macrophages

Resumo

Durante as últimas décadas, as infeções fúngicas têm emergido como doenças de elevado risco para a vida humana, principalmente devido ao aumento da população imunocomprometida. Por esta razão, *Alternaria infectoria* revela-se como um agente patogénico raro e oportunista, sendo o género *Alternaria* um dos fungos mais comuns no ar, o que por sua vez, pode originar várias manifestações de doença.

O sistema imunitário do hospedeiro é o principal determinante de quais serão as formas particulares de doença que se irão desenvolver após a exposição aos fungos. Tradicionalmente considerada apenas como a primeira linha de defesa, a imunidade inata recebeu recentemente renovada atenção, pois, apesar de uma certa falta de especificidade, nela reside a distinção entre próprio e não-próprio, eventualmente levando à ativação de mecanismos imunes adaptativos pela geração de sinais únicos.

Este trabalho teve o objetivo principal de caracterizar a resposta imune inata de macrófagos à presença de *A. infectoria*. No âmbito deste objetivo mais amplo inclui-se o estudo da interação entre os esporos de *A. infectoria* e macrófagos, assim como o papel dos recetores de adenosina A_{2A} na resposta do macrófago à infeção com esporos de *A. infectoria*.

A conclusão mais importante tirada deste trabalho é que os esporos de *A. infectoria*, não desencadeiam uma resposta pró-inflamatória em macrófagos. Em primeiro lugar, não foi encontrado um aumento na produção e libertação de TNF-α durante a infeção de macrófagos por esporos de *A. infectoria*. Em segundo lugar, a expressão do gene Adora 2a não se alterou com a infeção de macrófagos por esporos. E em terceiro lugar, os níveis de ATP extracelular não aumentaram substancialmente com a infeção. Além disso, o reconhecimento pelos macrófagos de esporos *de A. infectoria* demonstrou ser independente da sinalização de TLR2, enquanto os recetores de adenosina A_{2A} se acumularam em grupos durante a infeção com esporos. Concluiu-se também que, embora a fagocitose de esporos por macrófagos seja um processo muito rápido, por um lado a germinação em esporos internalizados não é retardada, por outro não ocorre a paragem da divisão celular de macrófagos, apesar de conterem esporos internalizados.

Quanto mais se descobre sobre as interações entre fungos e o sistema imunitário, melhor são as probabilidades de desenvolver antifúngicos mais eficazes.

Palavras-chave: *Alternaria infectoria*, conidia, macrófagos, resposta imunitária inata

Chapter 1

Introduction

1. Introduction

Nowadays, fungal infections are life-threatening and emergent diseases, mainly due to the increase of the immunocompromised population. For this reason, *Alternaria infectoria* comes forth as a rare opportunistic pathogen, which by being one of the most common airborne particles, can give rise to numerous manifestations of human disease.

In order to introduce this work, a general overview of the scientific literature regarding fungi and in particular *A. infectoria* will be given first. Secondly, a comprehensive description of the innate immune response to fungal infections will be addressed. In particular, how fungal recognition by host innate immune cells is achieved, as well as how do host cells distinguish between self and non-self stimuli. Finally, emphasis will be given to the role of endogenous signal molecules and their respective receptors in an ongoing fungal infection.

1.1. Fungi

The kingdom Fungi comprises many species that are associated with a wide spectrum of diseases in plant and animals. Fungi are heterotrophic eukaryotes that are traditionally and morphologically classified into yeast and filamentous forms. Most fungi are ubiquitous in the environment and have been estimated to comprise approximately 25% of the global biomass (Eduard, 2009). Additionally, humans are exposed by inhaling spores or small yeast cells, leading to distinct interactions between fungi and hosts, such as the establishment of symbiotic, commensal, latent or pathogenic relationships. Furthermore, their ability to colonize almost every niche within the human body requires specific reprogramming events that enable them to adapt to environmental conditions, fight for nutrients and even exploit stresses generated by host defence mechanisms (Romani, 2011).

The clinical relevance of fungal diseases has increased enormously in the second half of the twentieth century, mainly because of the increasing population of immunocompromised hosts (in part due to acquired immunodeficiency syndrome (AIDS), organ transplantation, chemotherapy and autoimmune diseases). Moreover, it has been predicted that global warming will enhance the number of fungal infections in mammals.

The crude mortality from opportunistic fungal infections still exceeds 50% in most human studies, and has been reported to be as high as 95% in bone-marrow transplant recipients infected with *Aspergillus fumigatus*. What is more, since fungal pathogens are eukaryotes, and therefore share many of their biological processes with humans, many antifungal drugs are highly toxic to humans when used therapeutically (Romani, 2004).

Introduction

1.1.1. Fungal Cell Wall

Among the eukaryotes, cell walls are found in many plant, fungal and algal species. The fungal cell wall is located outside de cell membrane and fulfils both protective and aggressive functions. Protection, since it acts as an initial barrier that is in contact with hostile environments encountered by the fungus. Besides, it also provides an aggressive function, as it harbours many hydrolytic and toxic molecules, most of them being in transit in the cell wall and required for a fungus to invade and prosper (Latgé, 2007; Casadevall *et al.*, 2009).

One essential but often unrecognized feature of the fungal cell wall is that it is a dynamic structure, continuously evolving and changing in response to the environment and during cell cycle (Latgé, 2010). Fungal cell walls are composed of a tight, semipermeable fibrillar network of polymers such as chitin, glucans polysaccharides and mannoproteins. Indeed, polysaccharides account for more than 90 % of the fungal cell wall.

However, in spite of its essential role, the cell wall of most fungi remains insufficiently studied and its biosynthesis incompletely understood, especially among filamentous fungi. This is a consequence of the technically impossibility of analysing the cell wall polymer without prior enzymatic or physicochemical treatment of the cell wall. Moreover, the current methodologies used to identify and characterize the fungal cell wall constituents are strong chemical treatments, which in the end do not provide insights about the distribution and localization of specific polysaccharides, since they destroy this particular three-dimensional (3D) polysaccharide network of the fungal cell wall (Latgé, 2007).

For almost all fungi, the central core of the cell wall is a branched β-1,3, 1,6 glucan that is linked to chitin via a β-1,4 linkage. Nevertheless, major differences have also been noticed among fungal morphotypes in the same species. For instance, many studies using fluorescent markers suggest that septa and apices have distinct structures to the lateral, older cell wall regions. Furthermore, the example of the conidium cell wall of *A. fumigatus*, which is covered by hydrophobins and melanin, in contrast with the exposure of α-1,3-glucans, galactomannan, galactosaminogalactan and N-glycosylated proteins on the surface of germinating conidia, further evidence the high variability of the fungal cell wall.

Overall, due to its vital biological role, unique biochemistry and structural organization and its absence in mammalian cells, the cell wall is an attractive target for the development of new antifungal agents.

1.2. *Alternaria*

1.2.1. Genus *Alternaria*

Alternaria is a very large and complex genus that holds several species of melanized hyphomycetes that cause opportunistic human infections, namely phaeohyphomycosis, a heterogeneous group of mycotic infections caused by dematiaceous fungi. Furthermore, *Alternaria* has a worldwide distribution, with many species being common saprophytes in soil, air and in a variety of other habitats. Additionally, some are ubiquitous agents of decay, plant pathogens and can also be found transiently on normal human skin and conjunctiva (Guarro, 2008). *Alternaria* infects mainly immunocompromised human hosts. In particular, *A. alternata* and *A. tenuissima* have been (erroneously) regarded as the most frequent species, primarily because species identification of these fungi is somewhat difficult due to their special sporulation growth conditions, subtle morphological differences (Figure 1), and the need for correct interpretation of their morphological features (Ferrer *et al.*, 2003). For instance, numerous cases of alternariosis have been attributed to *A. alternata* and *A. tenuissima*, when the actual causal agent was *A. infectoria*.
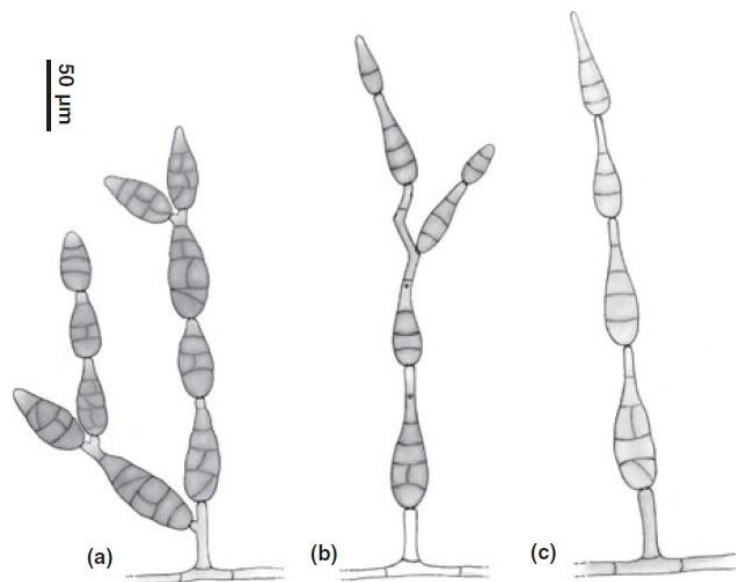
Figure 1. Morphology of conidia of: a) *Alternaria alternata*; **b)** *A. infectoria*; and **c)** *A. tenuissima* (Guarro, 2008).

1.2.1.1. Alternaria biological traits

In terms of biological traits, the genus *Alternaria* exhibits, septated and dark hyphae, while conidiophores are septated, of variable length and having sometimes a zigzag appearance. In addition, conidia are large (usually 8-16 x 23-50 µm) and brown, with both transverse and longitudinal septations (Larone, 2002). The formation of appressorium, an infection structure, is essential for penetration into host tissues and leads to the production of germ tubes during germination (Hwang *et al.*, 1995).

1.2.2. *Alternaria infectoria*

Alternaria infectoria is a rare opportunistic agent of phaeohyphomycosis, firstly described by E. G. Simmons in 1986. According to PubMed, only 46 articles can be found referring to "*Alternaria infectoria",* evidencing that the scientific literature regarding this specific organism is relatively scarce.

A. infectoria is a filamentous fungus (mould) that grows as branched multicellular filamentous structures (hyphae), which collectively form the mycelium. Moreover, *A. infectoria* exhibits long, dark conidophores, which are produced in strong branched chains owing to the formation of extended septated secondary conidia (spore) between conidophores (Thrane, 1996).

The number of reports describing clinical manifestations of human infections caused by *A. infectoria* has been rising in recent years. For example, in 2008, Hipolito *et al.* reported the first case of a phaeohyphomycotic brain abscess in a 5-year-old boy, in which the opportunistic agent turn out to be *A. infectoria* (Hipolito *et al.*, 2008). Besides, the increasing population of immunocompromised hosts allied to the daily exposure of humans by inhalation of *A. infectoria* conidia (one of the most prevalent fungal particles airborne), give rise to an unquestionable need for more knowledge regarding this organism and its role in human disease.

Since *A. infectoria* conidia are one of the most common fungal airborne particles, having already been associated with bronchial hyperresponsiveness (Nelson *et al.*, 1999; Murai *et al.*, 2012), an undeniable relationship between *A. infectoria* and asthma exists. Asthma, a chronic inflammatory disease, is one of the most common health afflictions worldwide, with approximately 300 million people suffering from this disease, 70% of whom have associated allergies (Murai *et al.*, 2012). Several epidemiologic studies have reproducibly shown that *Alternaria* sensitization is associated with allergic asthma. However, the mechanism of this specific association remains a scientific enigma (Gergen, 1992; Halonen *et al.*, 1997; Arbes *et al.*, 2007).

1.3. Innate Immune Response to Fungal Infections

The host immune system is a major determinant of which particular forms of disease will develop after exposure to fungi. Because human beings are continuously exposed to fungi, yet rarely develop fungal diseases, (except in circumstances of deliberate or primary immunodeficiency) it is clear that a stable host-pathogen interaction is a presumable condition for most pathogenic fungi. Nevertheless, this condition requires that the induced immune response needs be strong enough to allow host survival with or without pathogen elimination, and to establish commensalism or persistency with no excessive proinflammatory pathology (Romani & Puccetti, 2007). The host defence mechanisms against fungi are numerous and range from protective mechanisms that were present early in the evolution of multicellular organisms (innate immunity) to refined adaptive mechanisms, which are specifically induced during infection and disease (adaptive immunity).

Traditionally considered only as the first line of defence, innate immunity has recently received renewed attention because, despite a certain lack of specificity, it effectively distinguishes between self and non-self, eventually leading to the activation of adaptive immune mechanisms by the generation of unique signals. The constitutive mechanisms of innate defence are mainly present at sites of continuous interaction with fungi and also include the barrier function of body surfaces and the mucosal epithelial surfaces of the respiratory, gastrointestinal and genitor-urinary tracts (Romani, 2011).

1.3.1. Macrophage interaction with fungi

The mononuclear phagocytic system consists of monocytes circulating in the blood and macrophages in the tissues. Differentiation of a bone marrow-derived monocyte into a tissue macrophage involves a complex number of changes. Macrophages are dispersed throughout the body, some take up residence in particular tissues, becoming fixed macrophages, whereas others remain motile and are so called free or wandering macrophages (Kindt *et al.*, 2007).

Host immune cells express pattern-recognition receptors (PRRs), such as toll-like receptors (TLRs) and c-type lectin receptors (CLRs), which detect pathogen-associated molecular patterns (PAMPs) in fungi. In fact, these PRRs on phagocytes (Figure 2) initiate downstream intracellular events that promote the activation of the immune system and the clearance of fungi. In addition, macrophages, which are professional phagocytic cells, mostly contribute to the antifungal innate immune response through phagocytosis, leading to the pathogen killing.
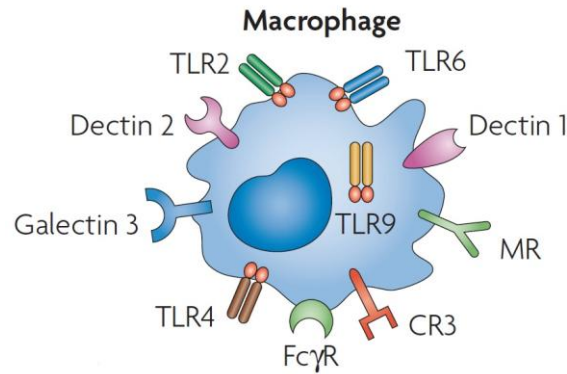
Figure 2. Macrophage pattern-recognition receptors involved in fungal recognition. The differential expression of pattern-recognition receptors by macrophages is shown. CR3, complement receptor 3; FcγR, Fcγ receptor; MR, mannose receptor; TLR, Toll‑like receptors. Adapted from Netea, Brown *et al.*, 2008.

1.3.1.1. Pattern-recognition receptors (PRRs)

The innate immunity employs a set of germ line-encoded receptors termed pattern-recognition receptors (PRRs) for sensing invading pathogens. The principal functions of PRRs include opsonisation, activation of complement and coagulation cascades, phagocytosis, activation of proinflammatory signaling pathways, and induction of apoptosis. However, the interaction of intact fungi with host phagocytes is complex, involving multiple PRRs (Figure 3), thereby hampering our knowledge of these sophisticated mechanisms of recognition.

Mammalian toll-like receptors (TLRs) are a family of highly conserved cellular receptors that mediate cellular responses to PAMPs, such as zymozan, phospholipomannan, O-linked mannans and fungal DNA. Recognition of fungi by TLRs triggers the induction of numerous cytokines and chemokines through the interaction with the adaptor molecule Myd88 (myeloid differentiation primary response protein 88). In contrast, the contribution of individual TLRs may vary depending on the fungal species, fungal morphotypes, route of infection and receptor cooperativity (Romani, 2004). For instance, signaling through TLR2 by zymozan occurs together with the receptor dectin-1, evidencing a collaborative recognition of distinct microbial components by different classes of innate immune receptors (Gantner *et al.*, 2003). Furthermore, TLRs facilitate the presentation of fungal antigens by dendritic cells (DCs) and tailor pathogen-specific T cell responses. This is in agreement with the role of TLRs in controlling fungal antigen processing and presentation during the simultaneous phagocytosis of self and non-self compounds (Blander & Medzhitov, 2006).

C-type lectin receptors (CLRs) are also essential for fungal recognition and for the induction of proper innate and adaptive immune responses; indeed, individuals with

genetic deficiencies in CLRs are highly susceptible to fungal infections (Romani, 2011). The main function of CLRs in fungal recognition is in the binding and subsequent internalization for direct pathogen elimination by phagocytes. At the same time, lysosomal degradation produces antigenic fragments that after presentation by macrophages to DCs stimulate the adaptive immune system.
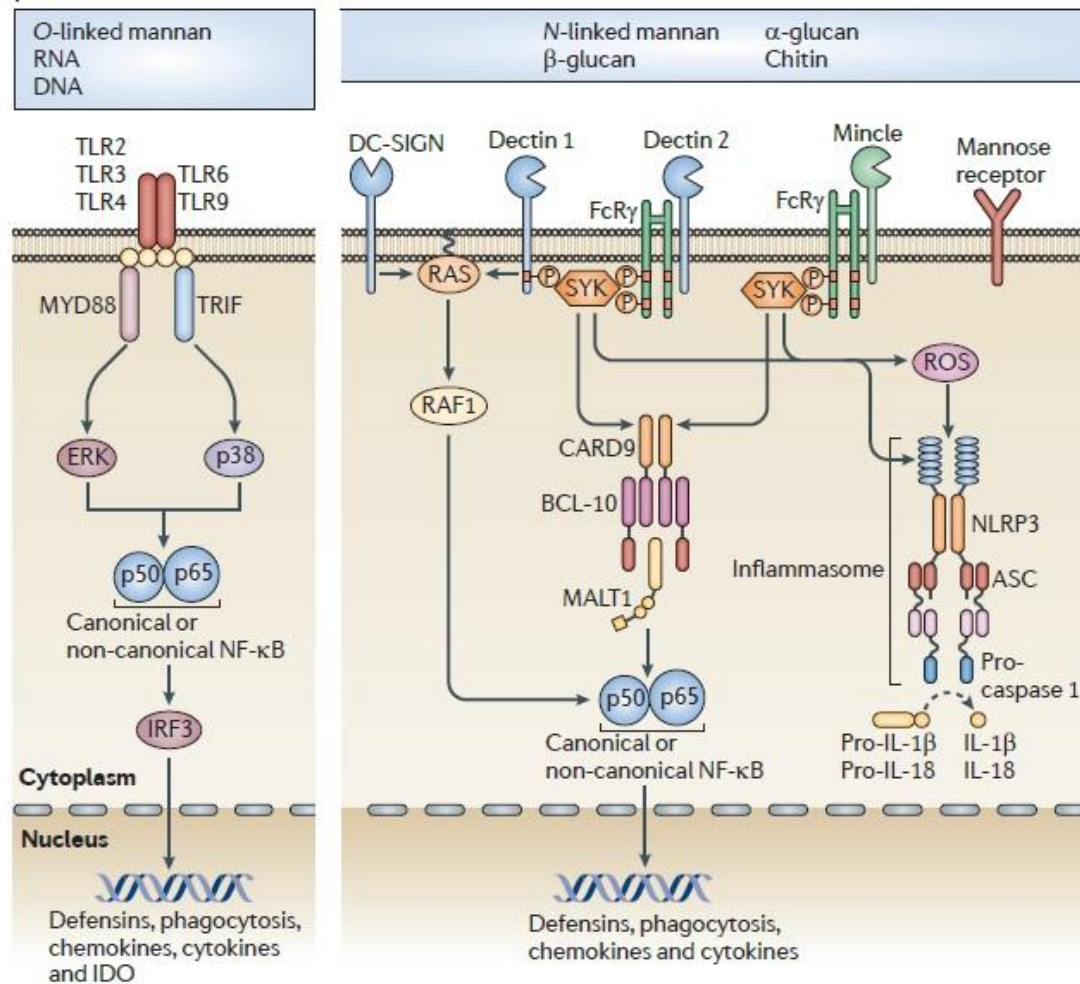
Figure 3. Signaling pathways in innate recognition of fungi. Pathogen-associate molecular patterns (PAMPs) that are present during fungal infections are recognized by pattern-recognition receptors (PRRs). The two major PRRs families are Toll-like receptors (TLRs) and C-type lectin receptors (CLRs; such as dectin-1, dectin-2, DC-SIGN, mincle, and the mannose receptor). TLRs and CLRs activate multiple intracellular pathways upon binding of specific fungal PAMPs, including β-glucans, chitin, mannans linked to proteins through N- or O-linkages and fungal nucleic acids. These signals activate canonical or non-canonical nuclear factor-κB (NF-κB) and the NLRP3 inflammasome, and this culminates in the production of defensins, chemokines, cytokines, reactive oxygen species (ROS) and indoleamine 2,3-dioxygenase (IDO). ASC, apoptosis-associated speck-like protein containing a Card; BCL-10, B cell lymphoma 10; Card9, caspase recruitment domain-containing protein 9; ERK, extracellular signal-regulated kinase; FcRγ, Fc receptor γ-chain; IL, interleukin; IRF3: IFN-regulatory factor 3; Malt1, Mucosa-associated lymphoid tissue lymphoma translocation protein 1; Myd88, myeloid differentiation primary response protein 88; Sky, spleen tyrosine kinase. Adapted from Romani, 2011**.**

The CLR family encompasses a number of PRRs, such as dectin-1 (also known as CLEC7A), dectin-2 (also known as CLEC6A), mincle (also known as CLEC4E), DC-

specific ICAM3-grabbing non-integrin (DC-SIGN), the mannose receptor (also known as macrophage receptor 1 (MR)), langerin (also known as CLEC4K) and the mannose-binding lectin. Undoubtedly, dectin-1 is the principal PRR that recognizes β-glucans. Thus, in response to fungi, it induces intracellular signaling via its cytoplasmatic immunoreceptor tyrosine-based activation (ITAM)-like motif both through a pathway involving spleen tyrosine (Sky) kinase, phospholipase Cγ2 (PLCγ2) and caspase recruitment domain-containing protein 9 (Card9), and also through the Raf-1 proto-oncogene serine/threonine-protein kinase pathway. Additionally, the Sky-Card9 pathway also activates the NLRP3 (NOD-, LRR- and pyrin domain-containing 3) inflammasome, which culminates in proteolitic activation of proinflammatory cytokines, such as interleukine-1β (IL-1β) and IL-18 by caspase 1 (Brown, 2011).

1.3.1.2. Fungal pathogen-associated molecular patterns (PAMPs)

The fungal cell wall can be described as a dynamic, highly organized organelle that determines both the shape and viability of the fungus (van de Veerdonk *et al.*, 2008). In addition, the fungal cell wall is predominantly composed of carbohydrate polymers interspersed with glycoproteins. The three major components, found in all medically important fungi studied to date are β-glucans (polymers of glucose), chitin (polymer of N-acetylglucosamine) and mannans. Even though these three components are intermingled throughout the cell wall, chitin tends to be found predominantly near the plasma membrane, while mannans have a propensity for the outer cell wall (Levitz, 2010). The central core of the cell wall is composed by branched β-1,3-glucan cross-linked to chitin (Latgé, 2007).

Despite this general overview of the fungal cell wall, it is, nevertheless, important to emphasize that extensive differences may be found when comparing different fungal species, even when comparing strains within a species. Also, differences are found between hyphae and conidia cell wall (Latgé, 2010). In fact, many fungi, namely *A. infectoria*, exhibit a fourth major component, melanin. The presence of melanins in fungi has been known since the early 1960s and several studies (Jacobson, 2000; Gomez & Hamilton, 2002) have already uncovered evidences that fungal melanins play an important role in fungal pathogenesis (Casadevall *et al.*, 2000).

Moreover, since cell wall components are fungal-specific, they are ideal targets for recognition as non-self by the previously described PRRs (Table I).

Table I. Examples of fungal cell wall ligands and their respective receptors.

Fungal Cell Wall Ligands	Receptors
β-1,3-glucans	Dectin-1
	CR3
Mannans	Mannose Receptor (CD206)
	DC-SIGN
	Dectin-2
Phospholipomannan	TLR2
O-linked mannoses	TLR4

1.3.1.3.   Damage-associated molecular patterns (DAMPs)

Host PRRs not only recognize PAMPs but also damaged host cell components, such as nucleic acids, alarmins and other molecules, collectively known as damage-associated molecular patterns (DAMPs) or endogenous danger signals (Bianchi, 2006).

Adenosine 5'-triphosphate (ATP), is primarily known for its function as an energy source in all cells, yet, it has also unique features as a DAMP, such as availability in high concentrations within the cytoplasm of every cell; low, almost negligible, levels in the extracellular space in healthy tissues; quick release following cell damage; and inactivation by powerful ubiquitous ecto-ATPases, making ATP a crucial signaling molecule (Willart & Lambrecht, 2009). In addition, extracellular ATP induces a variety of physiological responses in various cell types, via G protein-coupled P2Y receptors and P2X7 receptors. For example, it has been shown that lipopolysaccharides (LPS) stimulation of macrophages is accompanied by the release of ATP (Zhang & Mosser, 2008). Moreover, ATP acts as an endogenous danger signal, also contributing to cellular responses to pathogens, through production and release of proinflammatory mediators, including cytokines (Corriden & Insel, 2010).

Adenosine is an ubiquitous purine nucleoside that accumulates extracellularly (its levels rising up to 200-fold) in response to metabolic stresses such as hypoxia and inflammation (Milne & Palmer, 2011). Extracellular adenosine levels increase following the release of adenosine from cells or as a result of extracellular catabolism of released adenine nucleosides (Haskó *et al.*, 2008). Furthermore, adenosine plays an important role as a messenger of excessive tissue damage, leading to the activation of protective responses against an exorbitant inflammatory state (Figure 4).

Additionally, in 2005, Sitkovsky and Ohta hypothesized that in the case of an established infection, adenosine, by having a short half-life *in vivo* and by acting in an autocrine or paracrine manner, could inhibit inflammation in the most injured and therefore adenosine-rich areas, while allowing the ongoing pathogen destruction in the neighbouring and "yet-to-be-injured" tissues (Sitkovsky & Ohta, 2005).
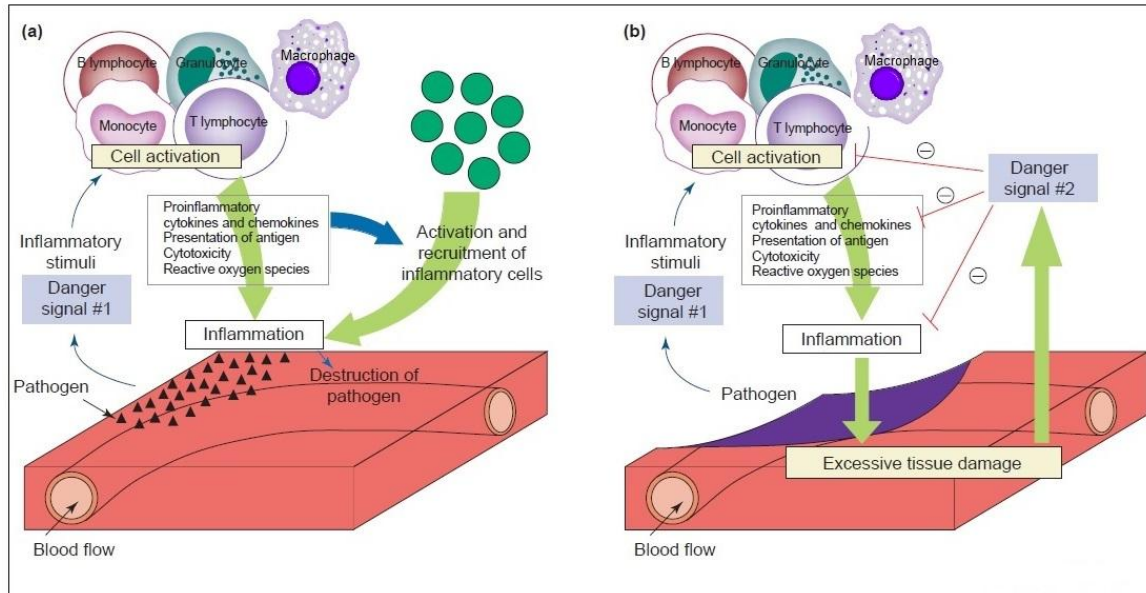
Figure 4. Two danger signal model of an immune response. a) When the presence of pathogen, injury or cell death is recognized (danger signal #1), immune cells are activated to initiate immune responses. Activated immune cells kill the pathogen, and expand inflammation by attracting and activating many other effector cells through the release of proinflammatory cytokines and chemokines. **b)** If inflammatory responses expanded uncontrollably, it might cause the loss of tissue function. To counteract excessive collateral tissue damage, specific signals are released from the damage tissue, which can evoke an anti-inflammatory response (danger signal #2). The outcome will be determined by a balance between proinflammatory signal #1 (e.g. pathogen load) and anti-inflammatory signal #2 (e.g. adenosine). Adapted from Sitkovsky & Ohta, 2005.

1.3.2. Macrophage immune response to fungal infections

1.3.2.1. Fungal Uptake

The recognition of fungi by PRRs leads to their internalization through the actin-dependent process of phagocytosis, whereby cellular membranes enclose the fungal particle, resulting in the formation of an intracellular vacuole called phagosome. Immediately after scission from the surface membrane, the newly formed phagosome is innocuous, as its limiting membrane resembles the plasmalemma from which it was derived, while its fluid-phase contents are a reflection of the extracellular medium. The phagosome then, matures through a number of sequential steps involving extensive vesicle fission and fusion events, largely with components of the endosomal network, leading to the development of the phagolysosome, a compartment with potent anti-microbial activities, in which the internalized fungus is killed and digested (Brown, 2011).

Therefore, phagocytosis *per se* is insufficient to mediate the destruction of microbes; yet, scission is followed by a rapid succession of biochemical modifications that convert the nascent phagosome into a potent microbicidal organelle that is central to both innate and adaptive immunity (Flannagan *et al.*, 2012).

1.3.2.2. Fungal Killing

A number of oxidative and non-oxidative mechanisms which work synergistically to kill extracellular and internalized fungi are employed by phagocytic cells. The activation of these activities is greatly influenced by the state of cellular activation, which is controlled mainly, but not exclusively, through the actions of cytokines and other mediators of inflammation. Different phagocytes exploit distinct strategies to kill or restrict fungal growth, and these activities are also dependent on the fungal species involved (Brown, 2011).

The production of reactive oxygen intermediates (ROI), also termed respiratory burst, is thought to be the major component of the anti-fungal defence mechanism of phagocytes. Moreover, it is mediated through a multi-component protein complex, the NADPH oxidase, which assembles at the phagosomal or plasmalemma membrane upon activation by cellular receptors, and then transfers electrons from cytoplasmatic NADPH to O_2, thereby producing superoxide. Although, superoxide by itself has limited, if any toxicity, it can be converted to toxic reactive oxygen intermediates, such as hydroxyl radicals and hydrogen peroxide (Brown, 2011).

Additionally, inducible nitric oxide synthase (iNOS), expressed in the plasma membrane after activation of macrophages by interferon-γ, constitutes the second major defence mechanism of classically activated macrophages (Pluddemann *et al.*, 2011).

Furthermore, mammals express a large variety of anti-fungal antimicrobial peptides (AMP), such as defensins, histatin 5, cathelicidins, cathepsins and other degradative proteases. Lysozyme, a phagolysossomal hydrolytic enzyme, has also been described as having a potent activity against fungi, mostly by killing or inhibiting fungal growth through the enzymatic hydrolysis of N-glycosidic bonds within the fungal cell wall and/or by injury of the cell membrane. Phagocytes can as well, restrict the nutrients availability. For instance, confining iron is essential for controlling many fungal infections and is achieved through sequestration by lactoferrin, down regulation of transferring receptors and by transporter proteins, which remove iron from the phagosome (Brown, 2011).

1.3.2.3. The role of A$_{2A}$ adenosine receptors in infections

The P1 class of purinergic receptors includes both adenosine receptors and P2 class of receptors that bind ATP. Purinergic receptors have been extensively studied since the early 1970s and have been implicated in a variety of physiological and pathological responses, such as T-cell effector function and initiation of immune cell activation. In particular, the A$_{2A}$ receptor appears to possess an extremely important role as sensor and terminator of proinflammatory activities and collateral tissue damage caused by overactive immune cells in response to infection (Sitkovsky & Ohta, 2005).

Adenosine receptor signaling is complex; in fact, it varies among receptor subtypes and also between the cells types involved. Moreover, the A$_{2A}$ receptor is a G$_s$ protein-coupled receptor, which, upon activation, induces an increase in the intracellular cAMP (cyclic adenosine monophosphate) concentration. Lastly, cAMP activates cAMP-dependent protein kinases.

Overall, the anti-inflammatory effects of A$_{2A}$ adenosine receptor (Figure 5) activation are mediated by: the activation of protein kinases that interfere with the inhibitor of κB kinase complex that selectively inhibits the nuclear factor κB (NF-κB) pathway, the activation of cAMP response element-binding protein (CREB), which mediates gene expression directly and indirectly by competing with the NF-κB pathway, and through the activation of the exchange factor activated by cAMP (EPAC) (Ramakers *et al.*, 2011).

Even though, a number of studies show that the A$_{2A}$ adenosine receptors have a role in the outcome of an established infection, in the case of a fungal pathogen it remains a mystery. Gradually, more research is being made with the aim of proving that this hypothesis holds true, in other words that A$_{2A}$ adenosine receptors exert a major anti-inflammatory effect during an ongoing fungal infection.
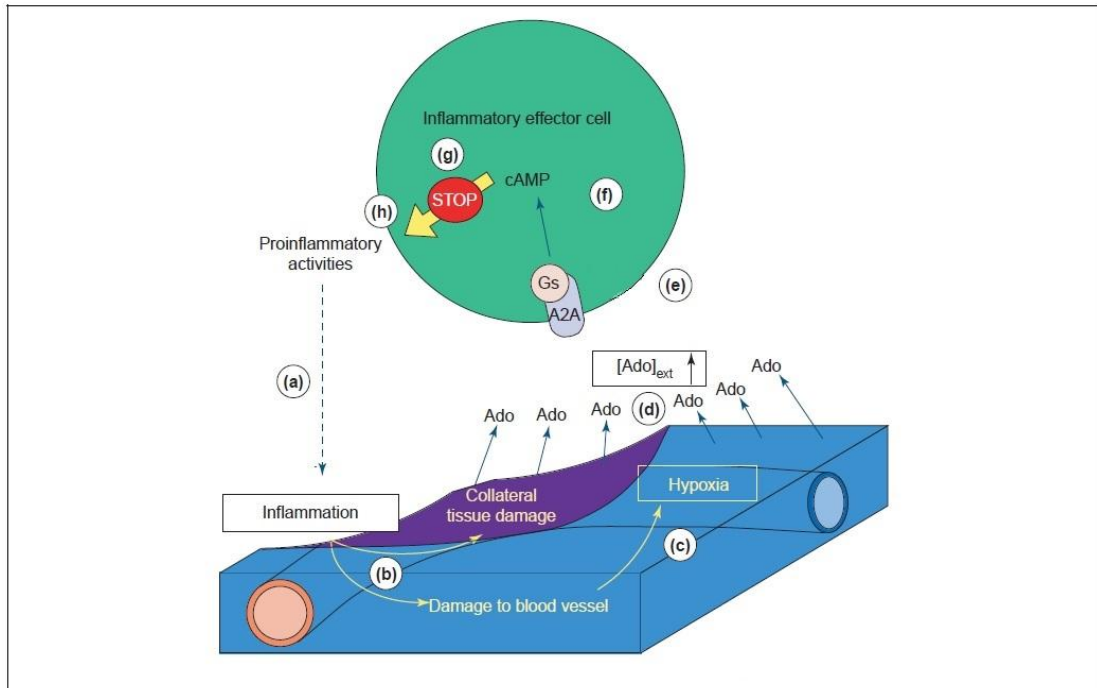
Figure 5. Danger signal triggers the delayed negative feedback inhibition of activated cells in inflamed tissues. a) The resident, recruited or tissue-surveying immune cells are activated to produce proinflammatory molecules (e.g. cytokines, reactive oxygen species) after the recognition of the fungal pathogen. **b)** This leads to the pathogen destruction even if some non-infected, bystander cells are also damaged collaterally. **c)** The collateral damage consequent of the continuous production of proinflammatory molecules, results in the interruption of blood supply and low oxygen tension (hypoxia). **d)** This local tissue hypoxia further conducts to the accumulation of extracellular adenosine (Ado), as a result of the hypoxia-associated decrease in intracellular levels of ATP, leading to an increase of AMP levels and the inhibition of adenosine kinase by hypoxia. **e)** The concentrations of extracellular adenosine will further increase and this, will determine the intensity of the danger signal through high affinity A_{2A} adenosine receptors (A_{2A}: blue). **f)** The sufficiently high extracellular adenosine levels will trigger the maximal activation of G_s protein coupled A_{2A} adenosine receptors and the accumulation of intracellular cAMP, which has strong immunosuppressive properties. **g)** The increased cAMP then strongly inhibits ongoing effector functions and prevents their triggering in the newly activated immune cells that have just arrived in the inflamed area. **h)** This delayed negative feedback mechanism might enable immune cells sufficient time to destroy the fungal pathogen but also to prevent additional collateral tissue damage by inhibiting the production of proinflammatory cytokines and cytotoxic molecules. Adapted from Sitkovsky & Ohta, 2005.

1.4. Aims

This work has the main goal of characterizing the innate immune response of macrophages to *A. infectoria* conidia, a rare yet opportunistic human pathogen. Included in this broader objective are the study of *A. infectoria* conidia-macrophage interaction and the role of A_{2A} adenosine receptors in the macrophage response to *A. infectoria* conidia infection.

Chapter 2

Materials and Methods

2. Materials and Methods

2.1. Fungal Strains

The IMF006 *A. infectoria* strain used in this study was obtained from CBS-KNAW Fungal Biodiversity Centre, Utrecht, The Netherlands (reference CBS 137.9).

2.1.1. Fungal Culture media and Solutions

Potato Dextrose Agar (PDA) (213400, Difco, BD) plates were used for fungal mycelia and conidia growth. The medium was prepared according to the manufacturer's instructions, sterilized by autoclaving (121ºC, 1.2 atm for 20 minutes) and distributed into petri dishes (Corning).

2.1.2. Fungal Growth conditions

The IMF006 strain was maintained on solid PDA medium at 30ºC with 8 hours cycles of exposure to a blacklight lamp (F15W T8BLB; Grainger) for at least 10 days before use.

2.1.3. *A. infectoria* conidia harvest

The harvest of *A. infectoria conidia* was accomplished by adding Dulbecco's modified Eagle's medium (DMEM; Sigma-Aldrich) to each plate containing the mycelia and conidia growth. By gently debonding the spores from the mycelia, a conidial suspension was obtained and then filtered through linen to remove hyphae fragments. Using a Neubauer haemocytometer, the conidia number was determined and a conidial suspension with a final concentration of 2.5×10^5 conidia/mL was acquired.

2.2. Infection Assays

2.2.1. Cell line

The macrophage cell line used in this research was the RAW 264.7 mouse macrophage cell line from the European Collection of Cell Cultures (ECACC catalog number 91062702; Salisbury, UK).

Materials and Methods

2.2.2. Cell Culture

The macrophage cell line was grown in Dulbecco's modified Eagle's medium (DMEM; Sigma-Aldrich) supplemented with 10% inactivated Fetal Bovine Serum (FBS; Life Technologies), 10 mM Hepes, 12 mM sodium bicarbonate and 11mg/mL sodium piruvate (S8636, Sigma-Aldrich).

The cell culture was maintained in 75 cm^2 flasks (Corning) using 25 ml of medium and in a humidified atmosphere with 5% CO_2 at 37°C. For routine maintenance in culture (passage), cells were seeded at a confluence of estimatingly 10% and grown to a confluence of approximately 70%. All the experiments here described were performed with cells between passages 11 and 15.

Phosphate Buffered Saline solution (PBS buffer: 10mM Na2PO4; 1,8mM KH2PO4; 137mM NaCl; 2,7mM KCl at pH 7.4) was used to wash the macrophage cells.

2.2.3. Infection assays

A. infectoria conidia and macrophage cells were grown as described in section 2.1.2 and 2.2.2, respectively. The macrophages were platted on 16 mm cover-slips, placed in 12-well multiwell plates (Corning) for 18h at 37° in a 5% CO_2 atmosphere. The macrophage number was determined with a Neubauer haemocytometer and applied a cell density of 2.5 x 10^5 cells/mL in DMEM (Sigma-Aldrich) medium supplemented with 10% inactivated FBS (Life Technologies), 10 mM hepes, 12 mM sodium bicarbonate and 11 mg/mL sodium piruvate (S8636, Sigma-Aldrich). The expected macrophage density at the day of infection would be approximately of 5 x 10^5 cells/mL.

Prior to infection, *A. infectoria* conidia were harvest has described in section 2.1.3. The macrophage cells were washed twice with 37°C-pre-heated PBS and the culture medium renewed. *A. infectoria* conidia were added to RAW 264.7 cell cultures in a multiplicity of infection (MOI) of 1:2 (one spore to two macrophages).

2.2.3.1. Live Cell Imaging

So as to study the *A. infectoria* conidia-macrophage interaction, a live cell imaging approach was used.

Briefly, *A. infectoria* conidia and macrophage cells were grown as described in section 2.1.2 and 2.2.2, respectively, except that no 12-well multiwell plates with cover-slips were used. Instead, the cells were platted on a μ-dish$^{35mm, high}$ (81158, Ibidi). The infection assay was performed as described in section 2.2.3, with the exception that the MOI used was 1:4 (one spore to four macrophages).

The live cell imaging was performed in a Observer Z1 microscope (Carl Zeiss, Jena, Germany), with an objective Plan ApoChromt 20x | 0.8, with a coupled camera AxioCam HRm for four hours with one image per minute, at 37ºC. At least two independent experiments were conducted, and at least four movies were analysed from each experiment.

2.2.3.2. *A. infectoria* conidia-macrophage interaction assays

With the purpose of determining the percentage of internalized, adherent conidia and appressorium formation, infection assays as described in section 2.2.3 were performed. *A. infectoria* conidia and macrophage cells were grown as described in section 2.1.2 and 2.2.2, respectively.

After the desired time of infection, the 12-well multiwell plates were put on ice, while the cover-slips were washed twice with cold PBS and then fixed with 4% paraformaldehyde (533998, Sigma-Aldrich) in PBS for 12 minutes at room temperature. The fixed cells were again washed twice with PBS and then, the cover-slips were mounted on glass lamellae, using a fluorescent mounting medium, termed DAKO (DakoCytomation Fluorescent Mounting Medium) (S3023, Luso Palex Medical).

Images were acquired with Zeiss Axiovert 200 (Carl Zeiss), using a LD-A-Plan objective with 20x magnification. Lastly, cell count was achieved using ImageJ Plugging Cell Counter.

2.2.3.3. Mouse Tumour Necrosis Factor alpha (TNF-α) quantification by ELISA

With the purpose of quantifying the tumor necrosis factor alpha (TNF-α) production during the infection course, *A. infectoria* conidia-macrophage interaction assays were performed as describe above (section 2.2.3.), except that in these case no 16 mm cover-slips were added to the 12-well multiwell plate. Additionally, *A. infectoria* conidia and macrophage cells were grown as described in section 2.1.2 and 2.2.2, respectively.

At 0h, 30 min, 1h30min, 3h and 6h of infection, the 12-well multiwell plates were put on ice and 500 μL of the supernatants collected. Then, liquid nitrogen was used to freeze the samples. Finally, the samples were stored at -80ºC until further experiments.

With the purpose of quantifying the release of TNF-α, the commercially available Mouse TNF alpha ELISA Ready-SET-Go!® kit was used (88-7324, eBioscience®). The procedure was made, integrally, according to the manufacturer's instructions.

Firstly, the capture antibody solution was added to the 96-well multiwell plates and incubated overnight at 4ºC. Secondly, a set of washes with 0,05% Tween 20

Materials and Methods

(P5927, Sigma-Aldrich) in PBS was made and the wells were blocked 1 hour at room temperature with Assay Diluent. Then, a second set of washes with 0,05% Tween 20 in PBS was made and standards concentrations prepared. Both standards and samples were added to the wells and incubated for 2 hours at room temperature. Another set of washes was made; the detection antibody solution was added to the wells and incubated for 1 hour at room temperature. Subsequently, a set of washes was performed, followed by the addition of Avidin-HRP solution to the wells and incubated for 30 minutes at room temperature. Afterwards, the wells were washed and incubated for 15 minutes at room temperature with the TMB (tetramethylbenzidine) substrate solution. Lastly, the reaction was stopped with 1M H_3PO_4 (P6560, Sigma-Aldrich), and the plates were read in a spectrophotometer (SPECTRA MAX PLUS 384, Molecular Devices) at 450 nm and 570 nm. The reason for two readings at different wavelengths is because the manufacturer advises that the 570 nm absorvances should be subtracted to the absorbances at 450 nm.

2.2.3.4. Immunocytochemistry assay for TLR2, A_{2A} adenosine receptors, N-acetyl-D-glucosamine and sialic acid

In order to assess the presence and relative abundance of A_{2A} receptors, dectin-1 and TLR2 in RAW 264.7 cells during the course of infection with *A. infectoria* conidia, an immunocytochemistry approach was used.

Shortly, *A. infectoria* conidia and macrophage cells were grown as described in section 2.1.2 and 2.2.2, respectively. The infection assay was performed as described in section 2.2.3.

As a positive control of macrophage activation, 0,1 µg/mL LPS (Lipopolysaccharide from Escherichia Coli Serotype 026:B6; L-8274, Sigma-Aldrich) was added to the RAW 264.7 cell culture. After 30 min, 1h30min, 3h and 6h the 12-well multiwell plates were put on ice, while the cover-slips were washed twice with cold PBS and then fixed with 4% paraformaldehyde (S233998, Sigma-Aldrich) in PBS for 12 minutes at room temperature. The fixed cells were again washed twice with cold PBS, followed by a 10 minutes incubation in the dark with 0,01 mg/mL WGA (Wheat Germ Agglutinin) Alexa Fluor® 350 conjugate in PBS (W7024, Invitrogen), with the purpose of labelling both macrophages and conidia.

Next, permeabilization with 0,2% Triton X-100 (30632, BDH) in PBS for 10 minutes at room temperature was performed. Afterwards, macrophage cells were washed twice with PBS and then incubated with blocking buffer, 3% bovine serum albumin (BSA) (A3059, Sigma-Aldrich) in PBS, for 1 hour at room temperature, in order to block nonspecific labelling. At this point, incubation for 1 hour at 37 ºC with primary antibodies diluted in

3% BSA in PBS occurred: goat polyclonal antibody raised against A_{2A} receptors (1:400) (sc-7504, Santa Cruz Biotechnology Inc) and mouse monoclonal primary antibody raised against TLR2 (1:50) (sc-73361, Santa Cruz Biotechnology Inc). The cells were then washed thrice with PBS, in order to incubate with the appropriate secondary antibodies diluted in 3% BSA in PBS, for 1 hour at 37ºC: anti-goat Alexa Fluor® 647 (1:500) (A-21447, Invitrogen) and anti-mouse Alexa Fluor® 488 (1:200) (A-21202, Invitrogen).

Subsequently, another set of washes with PBS were performed and the cover-slips mounted on glass slides, using a fluorescent mounting medium, termed DAKO (DakoCytomation Fluorescent Mounting Medium) (S3023, Luso Palex Medical).

The cell imaging was performed on a Zeiss LSM 510 Meta Confocal Microscope, using a 63x Plan-ApoChromat (NA 1.4) oil objective.

2.2.3.5. Relative quantification of A_{2A} adenosine receptor gene (Adora 2a) expression in macrophages during *A. infectoria* conidia infection

With the purpose of quantifying the relative expression of the A_{2A} receptor gene (Adora 2a) in RAW 264.7 cells during the course of infection with *A. infectoria* conidia, a Real-Time RT-PCR approach was applied. The 18S rRNA gene was used as reference gene.

Shortly, *A. infectoria* conidia and macrophage cells were grown as described in section 2.1.2 and 2.2.2, respectively. The infection assay was performed as described in section 2.2.3, except that in this case no 16 mm cover-slips were added to the 12-well multiwell plate.

As a positive control of macrophage activation, 0,1 µg/mL LPS (Lipopolysaccharide from Escherichia Coli Serotype 026:B6; L8274, Sigma-Aldrich) was added to the RAW 264.7 cell culture.

After 30 min, 1h30min and 3h, the 12-well multiwell plates were put on ice and the cells were scraped and transferred to ice-cold eppendorf tubes (RNase free), centrifuged at 10,000 rpm, for 5 minutes at 4ºC (7500 33 25, Heraeus Biofuge Fresco). Subsequently, the pellet was resuspended in PBS and centrifuged at 10,000 rpm for 8 minutes at 4ºC. The obtained pellet was again resuspended in 100 µL cold (approximately 4ºC) PBS and stored at -80ºC until further experiments.

RNA extraction was performed using the RNA-Cell protocol of the Magna Pure Compact RNA Isolation Kit (04802993001, Roche) according to the manufacturer's instructions. Briefly, 100 µL of lysis buffer (provided by the kit) was added to the cell pellets (previously stored at -80ºC) and gently mixed, at room temperature. 200 µL of the late mixture were transferred to sample tubes and placed in the Magna Pure Compact Equipment. The RNA concentration and purity of the extracted samples was assessed,

Materials and Methods

using (Biophotometer®, Eppendorf) and followed by Reverse Transcription, using the Transcriptor First Strand cDNA Synthesis Kit (04896866001, Roche) according to the manufacturer's instructions. Firstly, in a sterile, nuclease-free eppendorf, the equivalent volume to obtain a final concentration of 10 ng/mL RNA was added, together with 2 µL of Random Hexamer Primer and RNase-free water (provided by the kit) were added to make up a total volume of 13 µL. Secondly, 4 µL of Transcriptor Reverse Transcriptase Reaction Buffer, 2 µL of Deoxynucleotide Mix, 0.5 µL of Protector RNase Inhibitor and 0.5 µL Transcriptor Reverse Transcriptase were added in a total final volume of 20 µL. Finally, the reverse transcription reaction was performed in a GeneAmp PCR System 2400 (PerkinElmer^{TM}), with the followed programme: 25ºC for 10 minutes, 50ºC for 60 minutes; 85ºC for 5 minutes, and lastly, completion at 4ºC.

Quatitative Real Time PCR was then perfomed using the LightCycler® FastStart DNA Master^{PLUS} SYBR Green I Kit (03515885001, Roche) according to the manufacturer's instructions. Firstly, a mixture comprising 10 µL of RNase-free water, 4 µL of LightCycler® FastStart DNA Master^{PLUS} SYBR Green I Master Mix, 0.5 µL of primer forward, 0.5 µL of primer reverse and 5 µL of the previously synthesized cDNA was added to the LightCycler® Capillarie (Roche). The final concentration of primer (A$_{2A}$ primers and as reference gene, 18S primers, as shown in Table II, used was 0.5 µM.

Table II. Oligonucleotides sequences used in quantitative Real Time PCR.

Gene	Primer	5'→ 3' sequence	Reference	Amplicon size (bp)
Adora 2a	Forward	CCGAATTCCACTCCGGTACA	(Bone *et al.*, 2010)	120
	Reverse	CAGTTGTTCCAGCCCAGCAT		
18S	Forward	CGGCTACCACATCCAAGGAA	(Marques *et al.*, 2006)	241
	Reverse	GCTGGAATTACCGCGGCT		

Secondly, the capillaries were assembled on the LightCycler® Sample Caroucel (Roche) and spinned using the LC Caroucel Centrifuge (Roche). Lastly, the LightCycler® Sample Caroucel containing the capillarie was placed on the LightCycler® II instrument and quantitative Real Time PCR performed (Roche, Portugal, Software LightCycler 2.0). The amplification was performed using the parameters shown in Table III.

Table III. Quantitative Real Time PCR parameters for amplification.

Gene	Step		Temperature (ºC)	Duration
Adora 2a	Initial Denaturation		95	10 minutes
	45 cycles	Denaturation	95	10 seconds
		Annealing	57	5 seconds
		Extension	72	5 seconds
	Cooling		4	∞
18S	Initial Denaturation		95	10 minutes
	45 cycles	Denaturation	95	10 seconds
		Annealing	55	5 seconds
		Extension	72	10 seconds
	Cooling		4	∞

Finally, the relative quantification data process was based on the ratio of Ct values corresponding to each gene for all samples and the corresponding reference gene. The Ct concerns the first cycle amplification, which corresponds to the cDNA fragment that was detected above the baseline. Thus, raw data were analyzed by relative quantification using the $2^{-\Delta\Delta Ct}$ method for each gene using the Ct values (Schmittgen & Livak, 2008).

An additional electrophoresis was performed using a 1% agarose gel, to separate the obtained quantitative real time PCR products. The band visualization was achieved by the Red Safe (IN 21141, Intron Biotechnology) labelling, which under UV light exhibits fluorescence.

2.2.3.6. Extracellular ATP quantification during *A. infectoria* conidia infection

In order to quantify the ATP release during the infection course, *A. infectoria* conidia-macrophage interaction assays were performed as describe above (section 2.2.3.), except that in these case no 16 mm cover-slips were added to the 12-well multiwell plates. Additionally, *A. infectoria* conidia and macrophage cells were grown as described in section 2.1.2 and 2.2.2, respectively.

After 30 min, 1h30min and 3h of infection, the multiwell plates were put on ice and the supernatants collected and transferred to ice-cold eppendorf tubes (RNase free), centrifuged at 10,000 rpm, for 2 minutes at 4ºC (7500 33 25, Heraeus Biofuge Fresco). The acquired supernatant was then stored at -80ºC until further experiments.

So as to quantify ATP from the supernatants collected previously, the Adenosine 5'-triphosphate (ATP) Bioluminescent Assay Kit (FL-AA, Sigma-Aldrich) was used. The

components of the kit were prepared as described in the manufacturer's instructions. Briefly, a standard curve was performed, and ATP quantification of the samples was carried out by adding 80 µl of each sample to a 96-well white plate (Corning). Each measure was made with three well intervals between each sample. 40 µl of ATP Assay Mix (provided by the kit) was then added to each well; the reaction was read in a VICTOR Multilabel Plate Reader (PerkinElmer^{TM}). This method relies on the consumption of ATP and the consequent emission of light when firefly luciferase catalyses the oxidation of D-luciferin. If ATP is the limiting reagent, the light emitted is proportional to the concentration of ATP.

2.3. Statistical Analysis

Statistical differences among several sample types were analyzed by the Student's two tailed t-test (unpaired test), in order to compare two groups. Significance values were indicated as $p < 0.05$, $p < 0.01$ and $p < 0.001$. At least three samples were used for three independent experiments. All results are presented as mean ± SEM with at least n=3.

For cell counting image processing, at least 1000 macrophages were count for each independent experiment. All cell counting results are presented as mean ± SEM with n=3.

Chapter 3
Results

3. Results

3.1. Live Cell Imaging

The Figure 6 shows a broad view of the infection of macrophages by *A. infectoria* conidia. These conidia were harvested as described under chapter 2 (materials and methods). In it, *A. infectoria* conidia exhibit differences both in the size and degree of colour (some conidia darker than others). Also, it is interesting to notice the different number of conidia inside each conidiphores, as described for this *Alternaria* species.
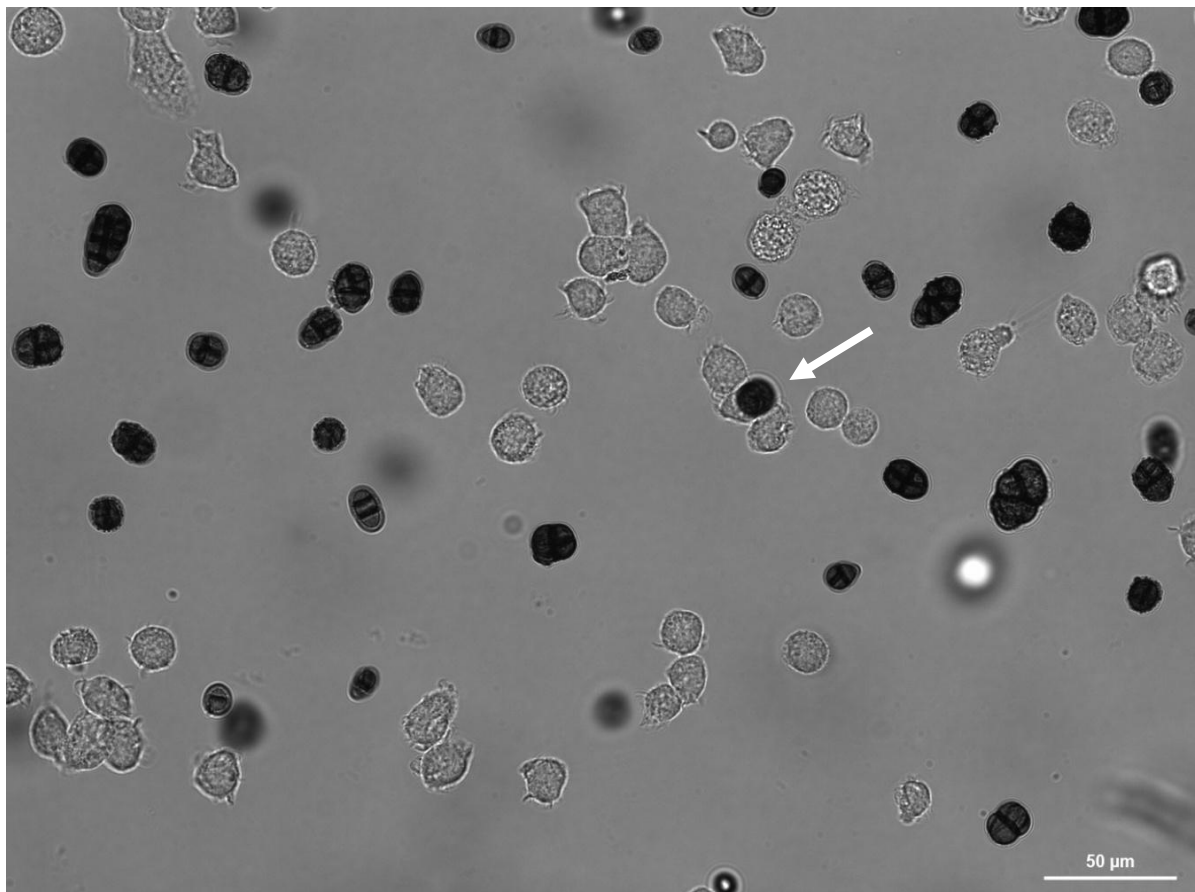
Figure 6. Representative live-cell video microscopy image showing RAW 264.7 macrophages infected by *A. infectoria* conidia at 0 h. White arrow indicates an internalized conidium. Scale bar indicates 50 µm. Image acquired in an Observer Z1 microscope (Carl Zeiss, Jena, Germany), with an objective Plan ApoChromt 20x | 0.8.

RAW 264.7 mouse macrophages show the typical morphology of innate immune cells, with no evidence of activation or contamination. Furthermore, at the time of image acquisition, which corresponds to 0 hours of infection, one conidium is already internalized by a macrophage (Figure 6, white arrow). This is a consequence of the technique's logistics, as the microscope settings, temperature conditions and finally, image acquisition cannot be made before the infection. Nonetheless, it is clear that the

majority of macrophages have not begun their function as phagocytes, either internalizing conidia or changing their morphology.

Macrophages are highly flexible and mobile cells (Figure 7). In fact, macrophages can exhibit a stretched and elongated form, which is in agreement with an ambulate state where the main goal is to look and catch foreign alleged pathogenic particles (in this case, *A. infectoria* conidia). Moreover, the figure shows an internalized conidium inside the macrophage, and surrounded by a membrane, the intracellular compartment termed phagosome. This is a rare event during *A. infectoria* spores infection.
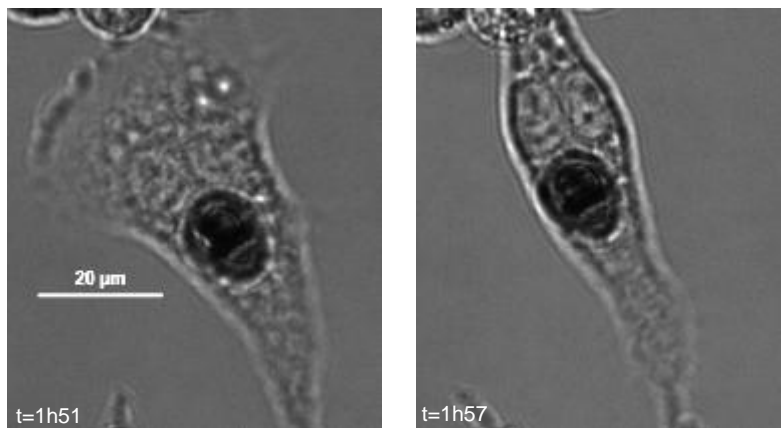
Figure 7. Macrophage extensive stretching with an internalized *A. infectoria* spore. RAW 264.7 macrophage exhibiting a stretched, elongated form. Scale bar indicates 20 µm. Images acquired in an Observer Z1 microscope (Carl Zeiss, Jena, Germany), with an objective Plan ApoChromt 20x | 0.8.

The macrophage can sense the presence of the *A. infectoria* conidia and is attracted towards it (Figure 8, a-k). Over the time, the macrophage comes nearer the spore, displaying its lamellipodia, eventually exhibiting pseudopod extensions to hold it. This is a very rapid process (time: 19 minutes). One observation during the course of infection assay was that once one macrophage internalizes one spore, more conidia seem to be attracted and adhere to the first macrophage (Figure 8, i-o).

The Figure 9 presents an interesting action of macrophages. It is firstly shown a macrophage (A) with an internalized *A. infectoria* spore plus three more adherent conidia (Figure 9, a). Later a second macrophage (B) approaches the first one (Figure 9, b-f) and grabs two of the three adherent conidia (Figure 9, g).

Also, it was observed that some macrophages while phagocytizing conidia, retain the ability to proceed to mitosis (Figure 10).
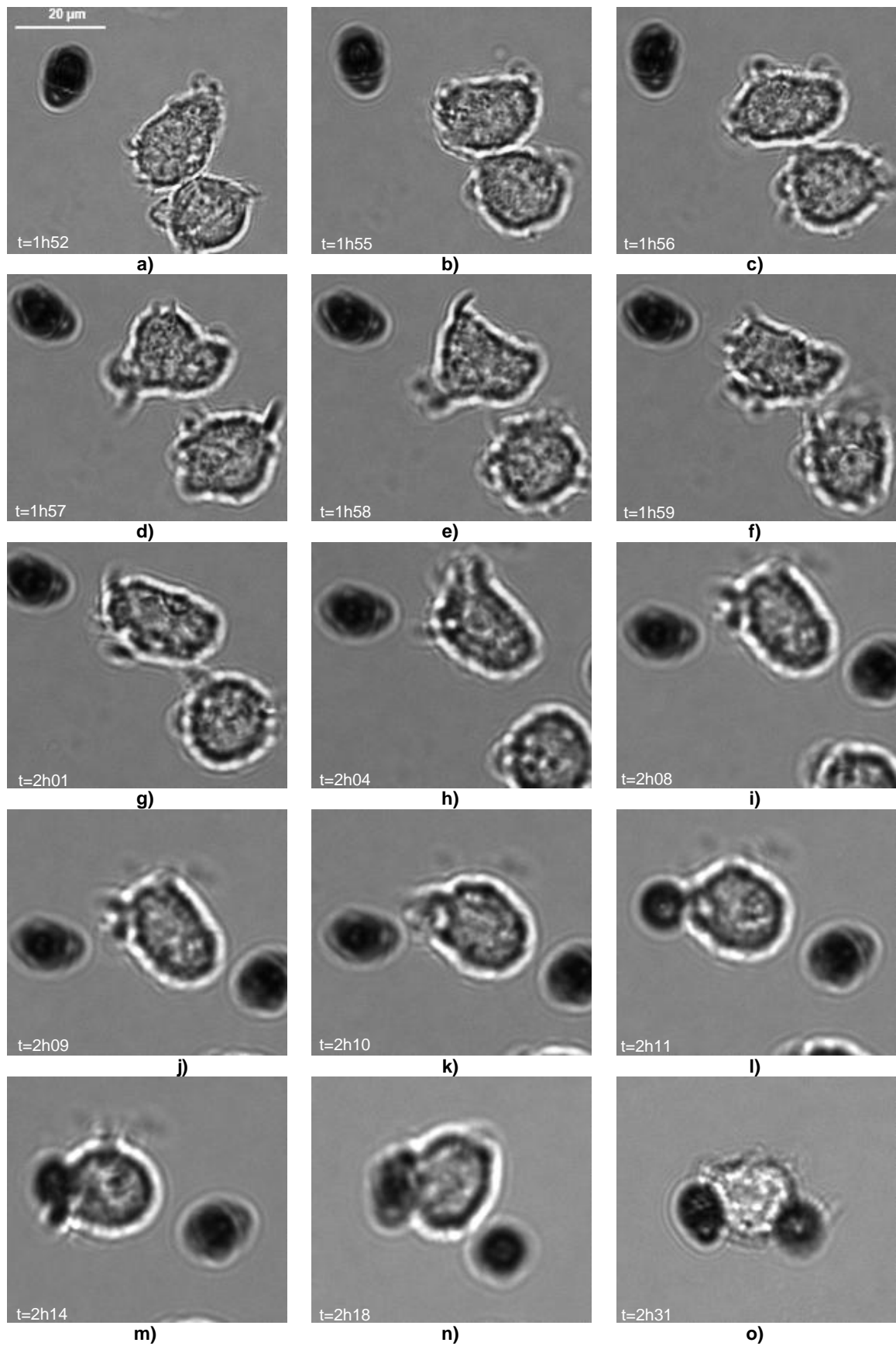
Figure 8. Phagocytosis/adherence of *A. infectoria* spores by a macrophage. Gradually, the macrophage approaches (exhibiting lamellipodia) the spore **(a-i)** and extends its pseudopod extensions in order to hold its target **(j-o)**. Scale bar indicates 20 μm. Images acquired in an Observer Z1 microscope (Carl Zeiss, Jena, Germany), with an objective Plan ApoChromt 20x | 0.8.

Results
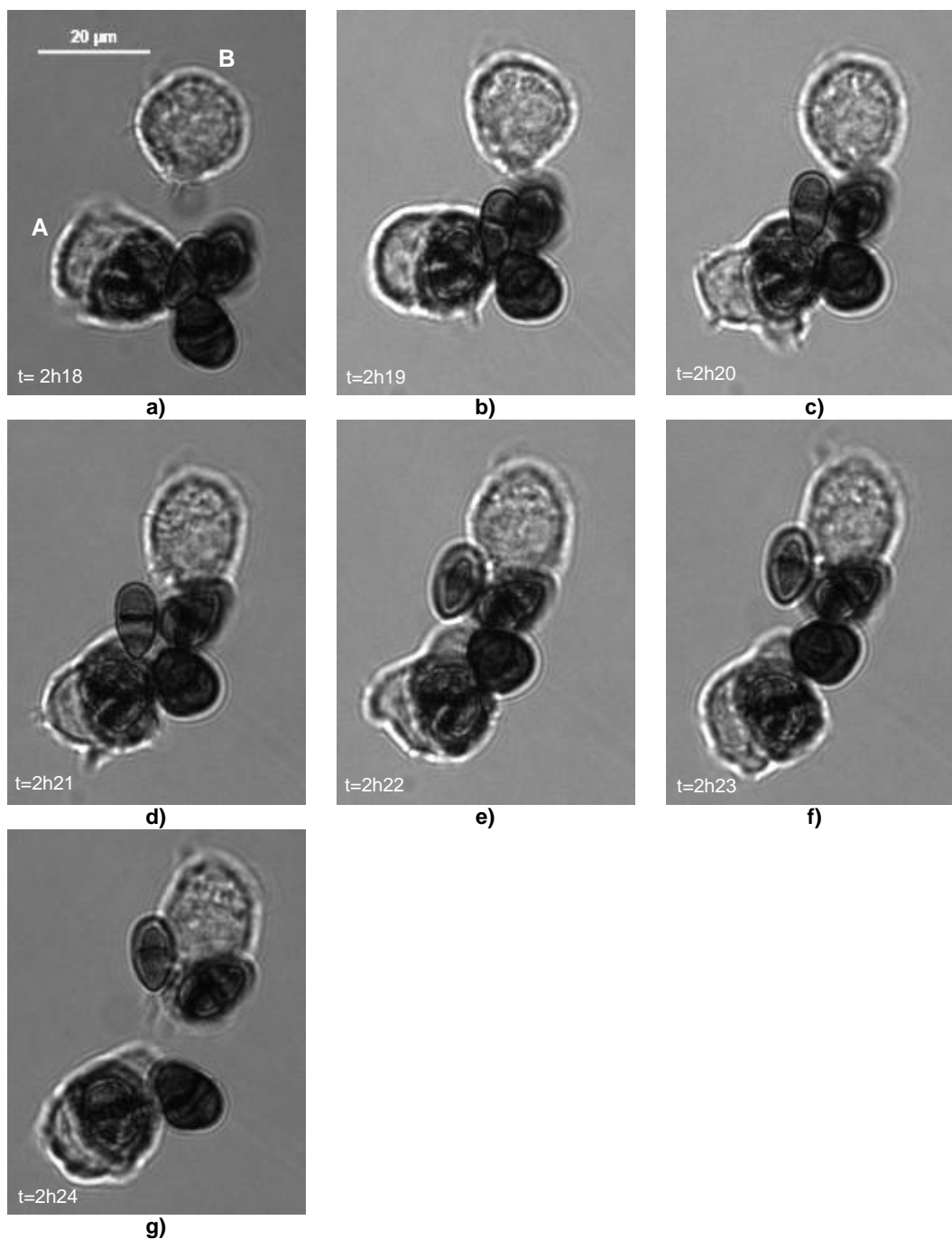
Figure 9. Cooperativity between macrophages during *A. infectoria* conidia infection. The macrophage A has already internalized one spore **(a)**, having three more adherents. The macrophage B approaches **(b-f)** and draws two of the three adherent conidia **(g)**. Scale bar indicates 20 μm. Images acquired in an Observer Z1 microscope (Carl Zeiss, Jena, Germany), with an objective Plan ApoChromt 20x | 0.8.
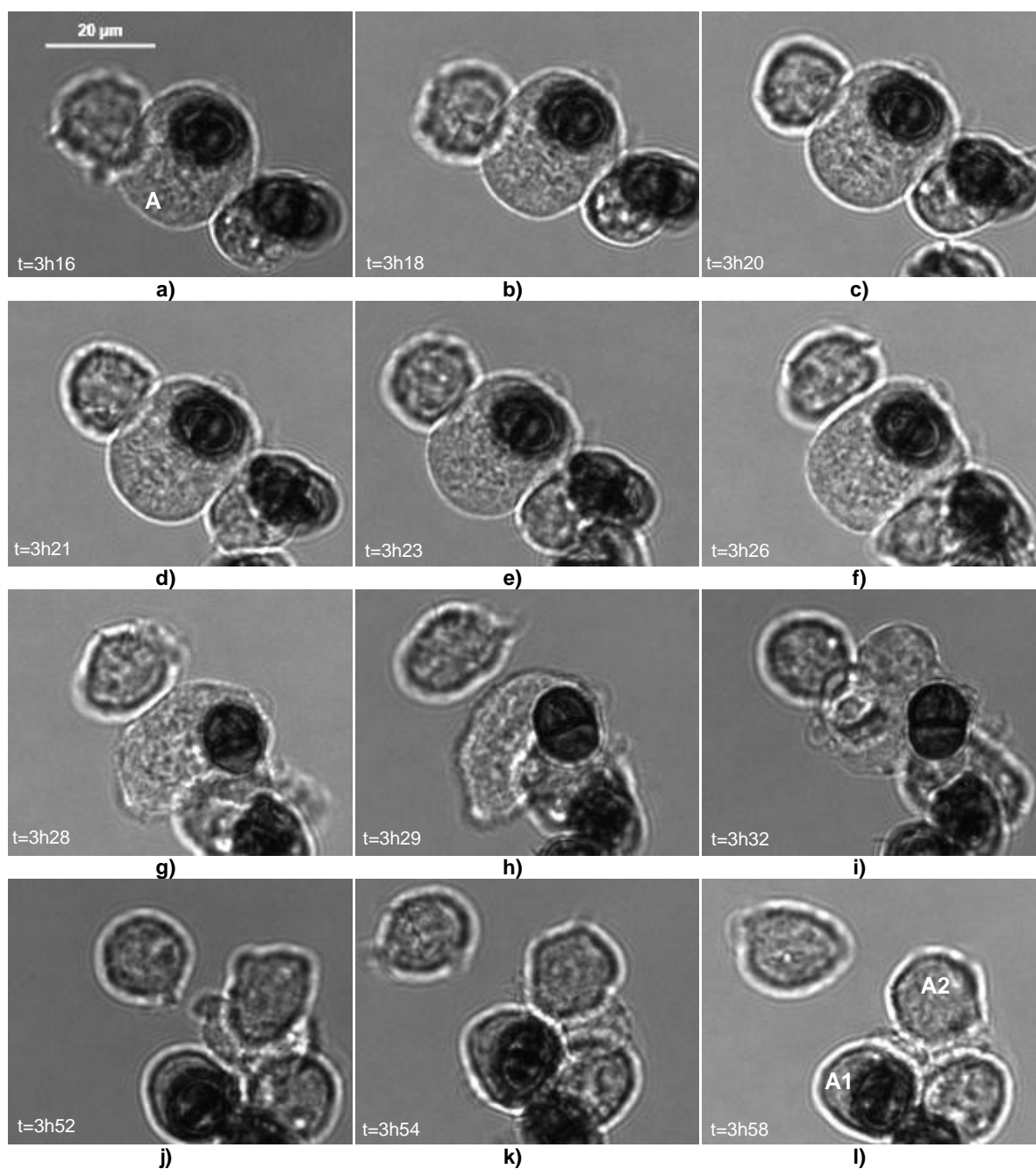
Figure 10. Macrophage division with internalized *A. infectoria* conidia. The macrophage A stars mitotic division **(a-h)** and originates two daughter cells (A1 and A2) **(l)**. Scale bar indicates 20 µm. Images acquired in an Observer Z1 microscope (Carl Zeiss, Jena, Germany), with an objective Plan ApoChromt 20x | 0.8.

Once the conidia adhere, and upon 4 h of assay, some conidia begin germinating (Figure 11). Although the conidium started germinating, the macrophage did not change its morphology (Figure 11).

In the same way as in Figure 11, Figure 12 shows over the time the germination of an adherent *A. infectoria* conidium. In addition, here is demonstrated the whole sequential process, starting with the formation of an appressorium.
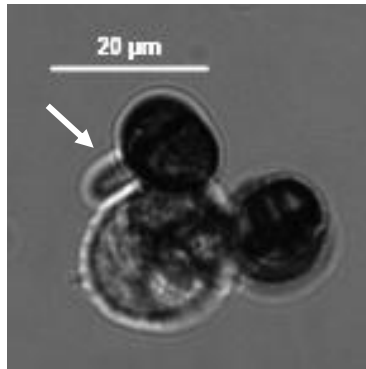
Figure 11. Adherent *A. infectoria* conidium germinating at 4 h of infection.
The white arrow indicates the appressorium formed. Scale bar indicates 50 µm.
Image acquired in an Observer Z1 microscope (Carl Zeiss, Jena, Germany),
with an objective Plan ApoChromt 20x | 0.8.
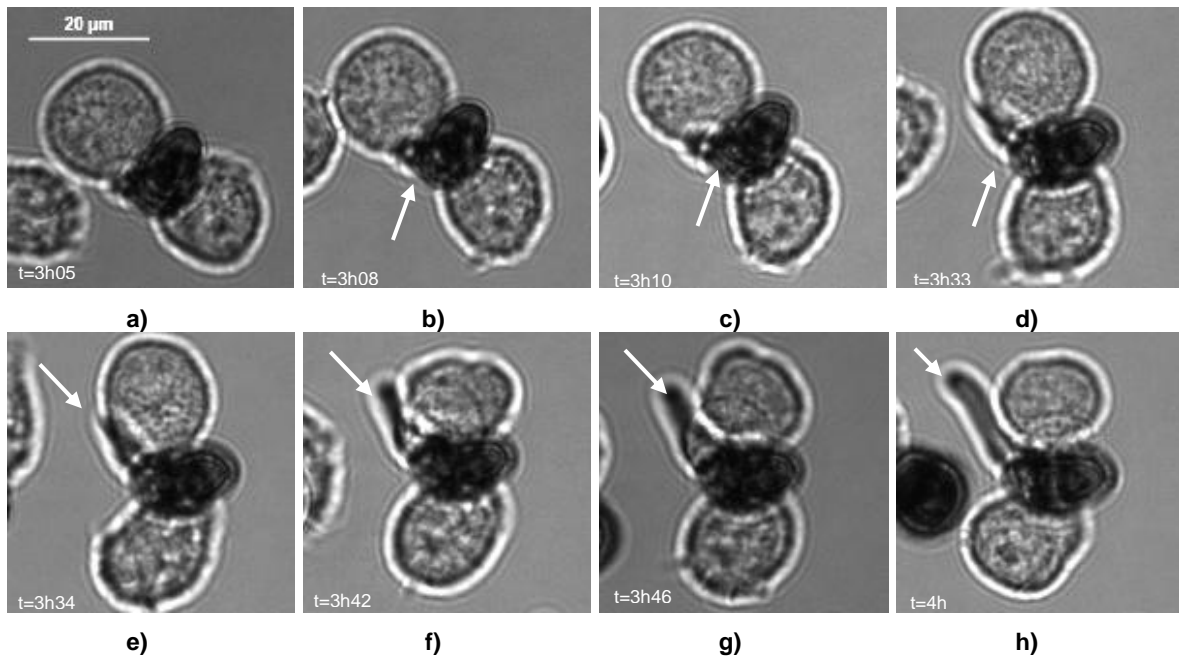
Figure 12. Appressorium formation in adherent *A.* infectoria conidium. White arrows indicate the
formed appressorium. Scale bar indicates 20 µm. Images acquired in an Observer Z1 microscope (Carl
Zeiss, Jena, Germany), with an objective Plan ApoChromt 20x | 0.8.

Also, an intracellular *A. infectoria* conidia germinating is shown (Figure 13). In this
case, the macrophage which internalized the conidia neither inhibits the formation of an
appressorium.
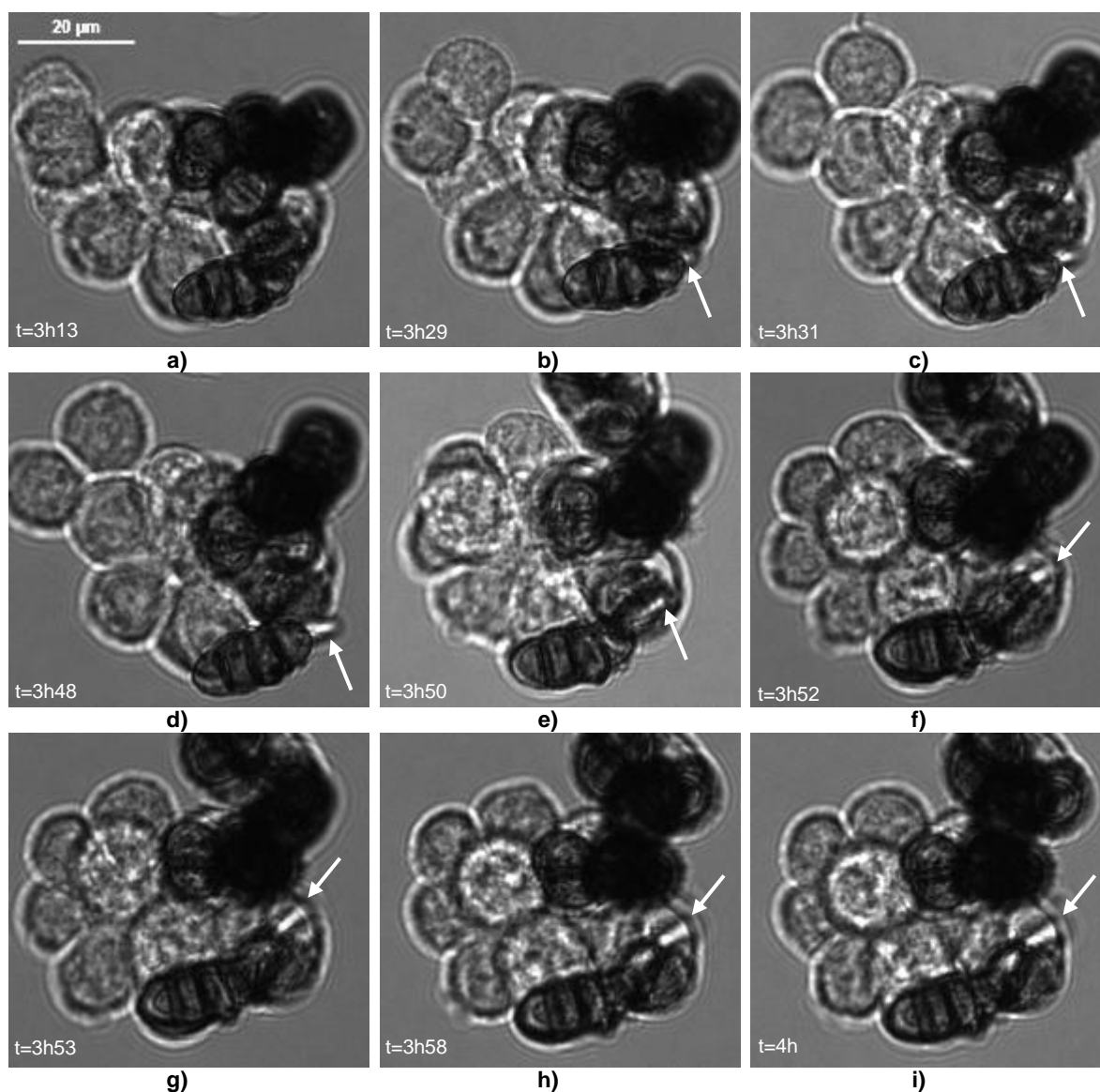
Figure 13. Appressorium formation in internalized *A. infectoria* conidia. An internalized spore starts germinating inside the macrophage. White arrows indicate the appressorium formed. Scale bar indicates 20 µm. Images acquired in an Observer Z1 microscope (Carl Zeiss, Jena, Germany), with an objective Plan ApoChromt 20x | 0.8.

Interestingly, it was observed a vesicular compartment inside the macrophage (Figure 14), which displays a smoother appearance, in contrast with the grainy aspect of the macrophage's cytoplasm. It seems that this compartment is localized next to the phagocytosed spore. Also, it is evidenced (as in Figure 13) the intracellular germination of the conidia.
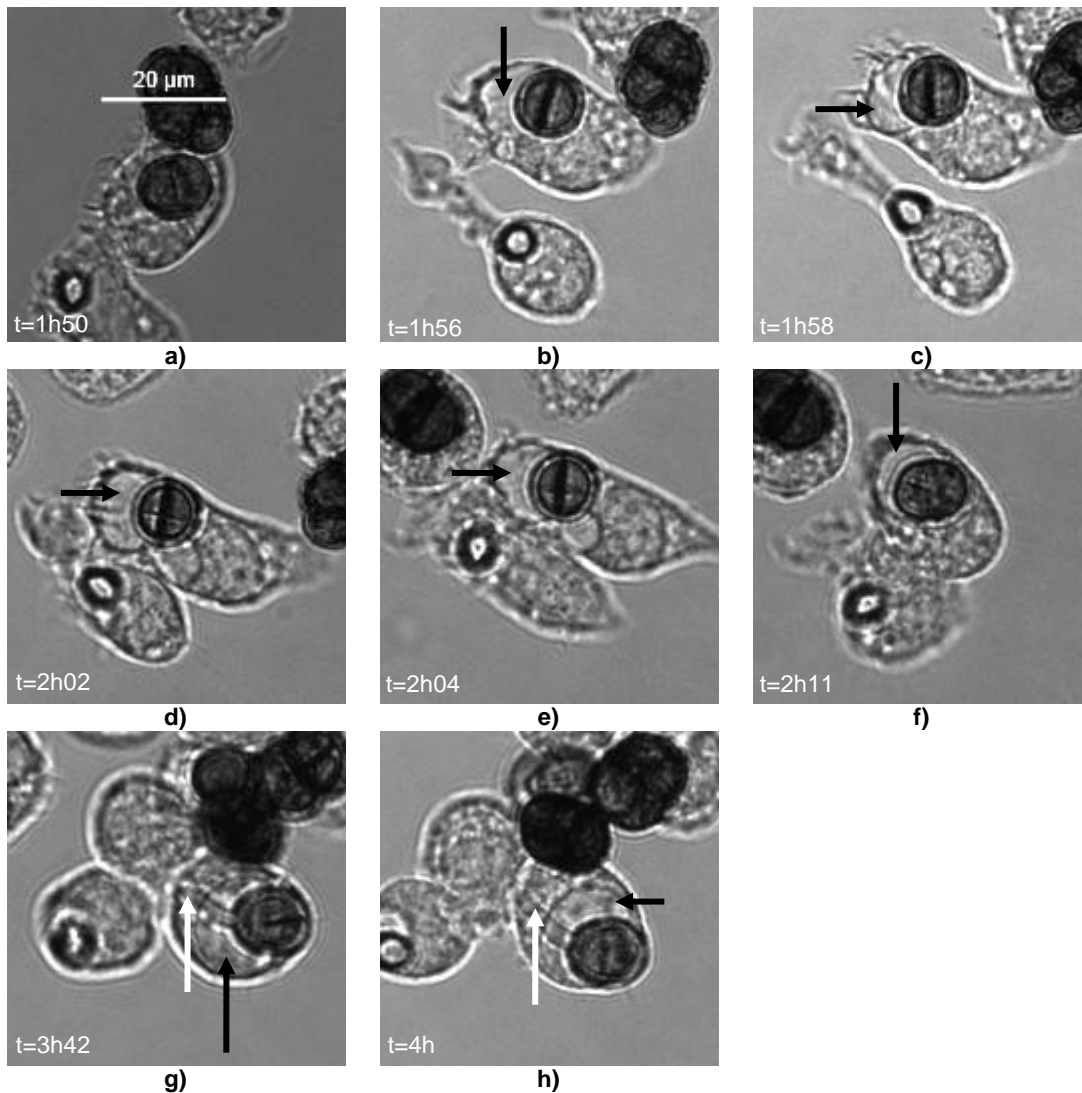
Figure 14. Compartment localized next to a phagocytosed and germinating _A. infectoria_ spore. Black arrows indicate the compartment, while white ones indicate the appressorium formed. Scale bar indicates 20 µm. Images acquired in an Observer Z1 microscope (Carl Zeiss, Jena, Germany), with an objective Plan ApoChromt 20x | 0.8.

## 3.2. Quantification of _A. infectoria_ conidia-macrophage interaction

In order to further characterize the macrophage response to _A. infectoria_ conidia, an understanding of the percentage of internalization, adhesion and appressoria formation was needed. For this, the microscopic images were used to count the number of conidia either internalized, adhered or conidia forming appressorium.

In what regards, the percentage of internalized _A. infectoria_ conidia by macrophages at several time checkpoints of infection (Figure 15). Indeed, at 30 min of infection it could be observed that almost 67% of the total number of conidia is internalized. Then, at 1h30min and 3 h of infection the percentage of internalized conidia decreases without statistical significance, and finally at 6 h of infection the percentage of

internalized conidia returns to 69%. This process, as already evidence by the live cell imaging, is a very fast process.

Furthermore, the percentage of adherent *A. infectoria* conidia (Figure 16), at 30 min of infection was approximately 17% of the total number of conidia. At 1h30min and 3 h of infection this value decreased to 10 and 1%, respectively. After 6 h of infection a minimum of 0.13% of adhesion was found. Meaning that the conidia were either internalized or free in the extracellular media.
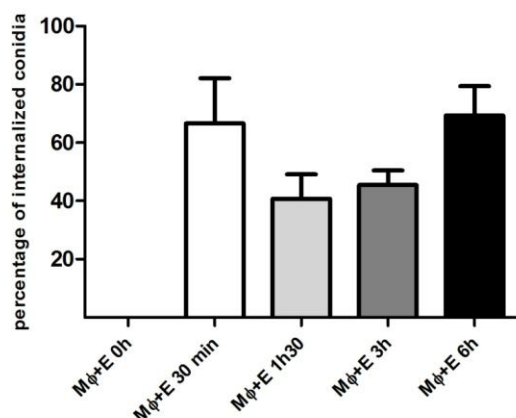
Figure 15. Percentage of internalized conidia. At 30 min of infection of macrophages (Mφ) with *A. infectoria* conidia (E), 66.7% of the conidia were already internalized. At 1h30min and 3 h of infection, a short reduction is noted. At 6 h a 69.3% of internalization is viewed. The results are presented as mean ± SEM, with n=3.
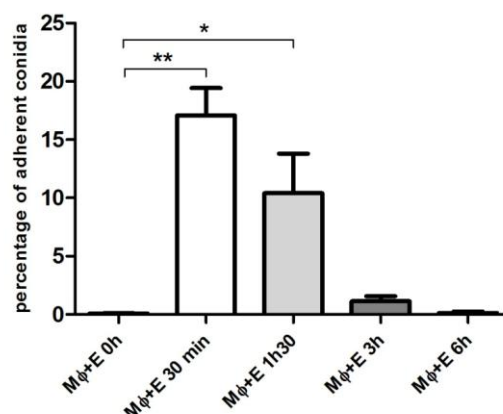
Figure 16. Percentage of adherent conidia. At 0 h of infection, 0.06% of the conidia (E) were adhered to macrophages (Mφ). At 30 min of infection, 17.1% of the total number of conidia was adhered to macrophages. After 1h30min, 3 h and 6 h of infection, the percentage of adherent conidia decreased to 10.4%, 1.1% and 0.13%, respectively. The results are presented as mean ± SEM, with n=3. *p<0.05; **p<0.01.

In terms of conidial germination, has shown in Figure 17, the percentage of appressoria formation over the time of infection, either in intra- and extracellular conidia, increased reaching at 6 h almost 6% of the total number of *A. infectoria* conidia.

The intracellular appressoria formation showed a lower rate of progression (Figure 18). At 30 min, 1h30min and 3 h of infection the percentage of intracellular appressoria formation is 0.3, 0.8 and 1%, respectively. However, at 6 h of infection 6% of the total number of conidia is germinating inside the macrophages, meaning that all conidia that were germinating were intracellular.
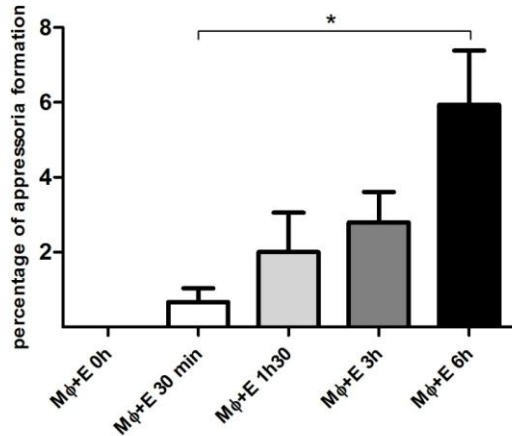
Figure 17. Percentage of appressoria formation. As the time of infection (of macrophages (Mφ) with *A. infectoria* conidia (E)) proceeds, the percentage of appressoria formation increases, reaching at 6 h of infection 5.93%. The results are presented as mean ± SEM, with n=3. *p<0.05.
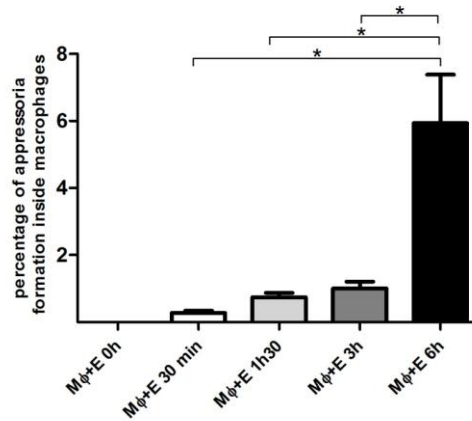
Figure 18. Percentage of intracellular appressoria formation. At 30 min of infection, 0.3% of the conidia (E) germinated inside the macrophages (Mφ). After 1h30min, 3 h and 6 h of infection, the percentage of appressoria formation increased to 0.8%, 1.0% and 5.93%, respectively. The results are presented as mean ± SEM, with n=3. *p<0.05.

3.3. TNF-α release in macrophages during the course of infection with *A. infectoria* conidia

Tumor necrosis factor alpha (TNF-α) is a proinflammatory cytokine released by several cell types such as macrophages, neutrophils and T lymphocytes. TNF-α promotes inflammation by a number of mechanisms, such as activation of nuclear factor kappa B, induction of interleukins (IL), as well as upregulation of migration of lymphocytes.

With the purpose of quantifying the production of TNF-α in the macrophage response to *A. infectoria* conidia, an ELISA was performed. Figure 19 shows that the concentration of TNF-α at 0 h and at 30 min of infection did not reach the detection limit indicated in the kit used (7.8 pg/mL), both for negative controls (macrophages), macrophages infected with *A. infectoria* conidia and positive controls (macrophages treated with lipopolysaccharides (LPS)). At 1h30min, LPS treated macrophages exclusively showed a TNF-α detectable level of 313 pg/mL. After 3 h of infection the negative control retain values below the detection limit, while macrophages infected by *A. infectoria* conidia displayed a slightly increase to 32 pg/mL and the LPS treated macrophages a more substantial one (608 pg/mL). Similarly, at 6 h LPS treated macrophages showed a considerable increase (987 pg/mL), whereas the macrophages infected by *A. infectoria* conidia exhibited a slightly decrease in TNF-α levels (13 pg/mL).

So, between 1h30min, 3 and 6 h a meaningful increase in TNF-α levels was observed, when RAW 264.7 cells were infected with *A. infectoria* conidia.

Overall, the response differences of TNF-α production in macrophages during the course of infection with *A. infectoria* conidia and macrophages treated with LPS are deeply distinct.
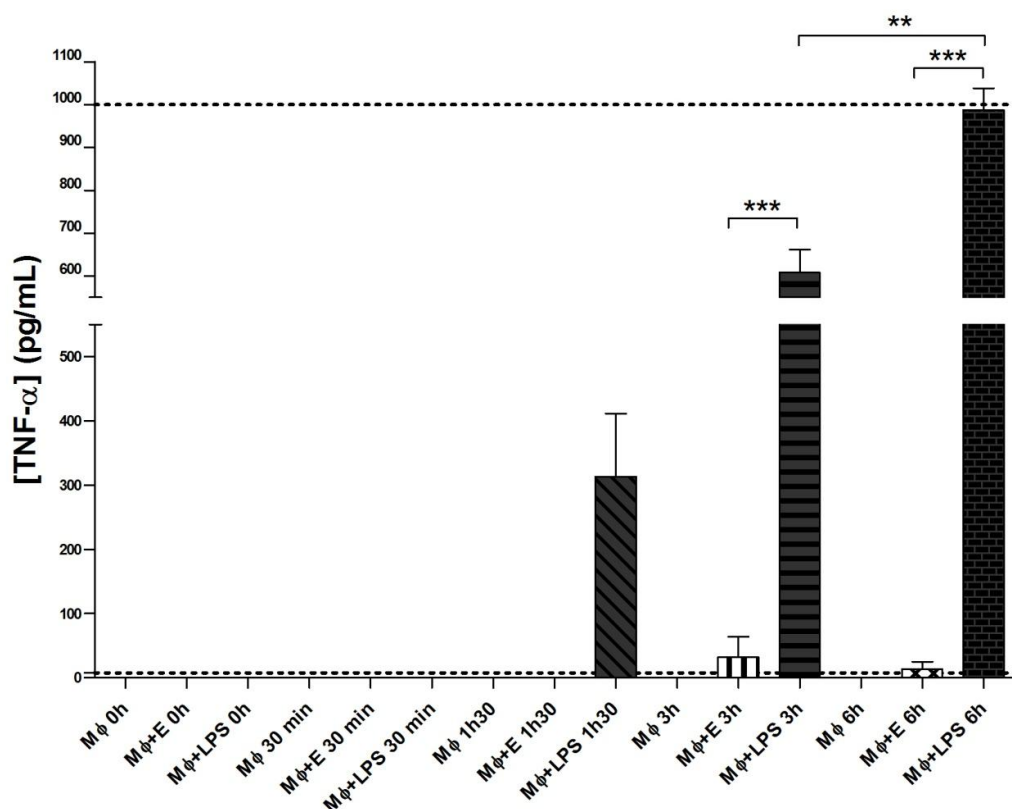
Figure 19. *In vitro* **TNF-α (Tumor Necrosis Factor-α) production by macrophages (Mɸ), macrophages in response to** *A. infectoria* **conidia (Mɸ+E) and macrophages treated with LPS (Mɸ+LPS).** Cytokine levels both in the absence of exogenous stimuli (negative control: Mɸ) and in the presence of conidia or LPS were at 0 h and 30 min below the detection limit (7.8 pg/mL). At 1h30min, only LPS treated macrophages showed detectable levels of TNF-α (313 pg/mL). After 3 h of infection the negative control retain values below the detection limit, while macrophages infected by *A. infectoria* conidia displayed a slightly increase (32 pg/mL) and the LPS treated macrophages a substantial one (608 pg/mL). Similarly, at 6 h LPS treated macrophages showed a considerable increase (987 pg/mL), whereas the macrophages infected by *A. infectoria* conidia exhibit a substantial decrease in TNF-α levels (13 pg/mL). The two dashed lines represent the bottom and upper limits of detection. The results are presented as mean ± SEM, with n=3. **p<0.01; ***p<0.001

3.4. Immunocytochemistry assay for TLR2, A_{2A} adenosine receptors, N-acetyl-D-glucosamine and sialic acid

The difficulty in seeing whether the spore is completely internalized by the macrophage cell led us to use wheat germ agglutinin that probes for N-acetyl-D-glucosamine and sialic acid.

The results showed that both spores and macrophages are marked by this probe; it was also revealed that hyphal tips were richer in N-acetyl-D-glucosamine and sialic acid, evidenced by the increase in fluorescence of those areas (Figure 20, white arrows).
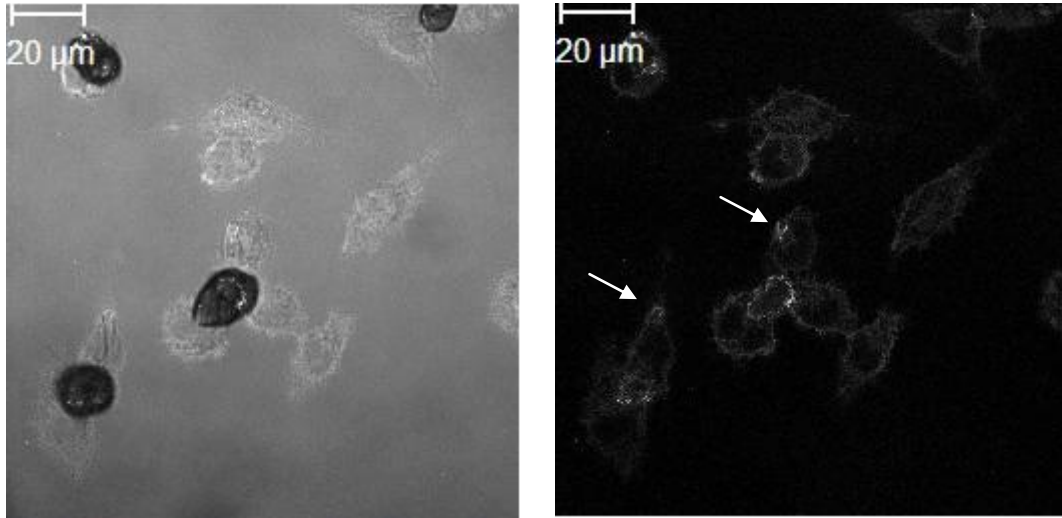
Figure 20. Labeling of macrophages infected by *A. infectoria* conidia with wheat germ agglutinin (WGA) Alexa Fluor® 350 conjugate (W7024, Invitrogen). Both macrophages and conidia exhibit staining. White arrows indicate hyphal tips. Scale bar indicates 20 μm. The cell imaging was performed on a Zeiss LSM 510 Meta Confocal Microscope, using a 63x Plan-ApoChromat (NA 1.4) oil objective.

Recognition of conidia by macrophages contributes to the fungal clearance as well as to the generation of a proinflammatory immune response. The initial contact is achieved by the presence of membrane bound pattern-recognition receptors (PRRs) such as toll-like receptor 2 and dectin-1. Furthermore, a later set of innate immune events take place, leading to the activation of other signaling cascades like the A_{2A} adenosine receptors activation. Therefore, the presence of toll-like receptor 2 and A_{2A} adenosine receptors in macrophages infected by *A. infectoria* conidia was assessed.

As Figure 21 shows no alterations of the localization or the amount of TLR2 were found when comparing macrophages and macrophages infected by *A. infectoria* conidia. Moreover, germination of an internalized conidium did not alter the basal quantity of TLR2 in the macrophage.

Mφ 1h30min

Mφ+E 1h30min

Mφ+E 1h30min
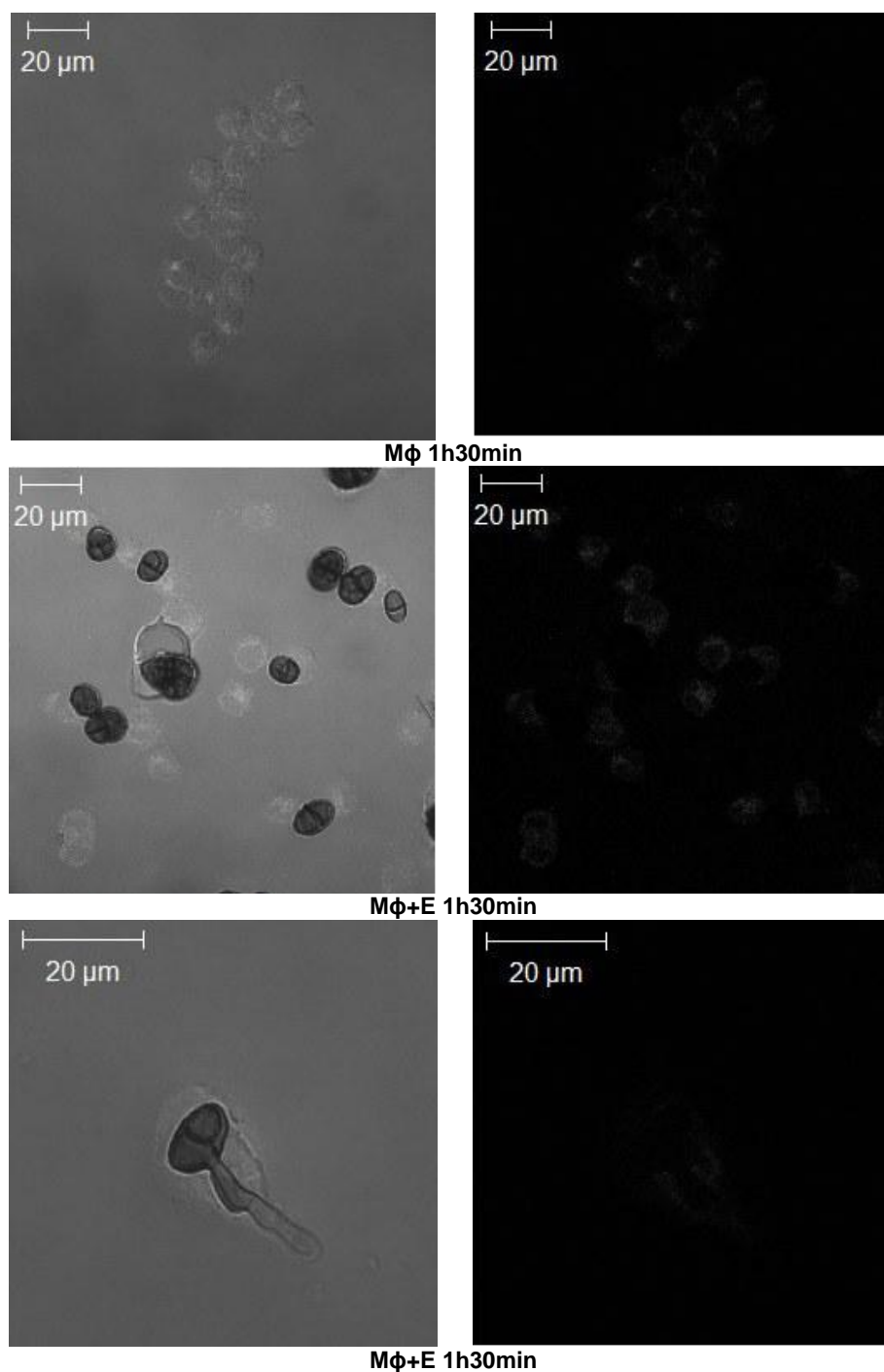
Figure 21. Toll-like receptor 2 immunolabeling during *A. infectoria* conidia infection. Both macrophages (Mφ) and macrophages infected by *A. infectoria* conidia (Mφ+E) exhibit the same profile of immunostaining. Also, no differences in the level of immunostaining were found when internalized conidium germinates. Immunocytochemistry was performed using a mouse monoclonal primary antibody raised against TLR2 (1:50) (sc-73361, Santa Cruz Biotechnology Inc) and anti-mouse Alexa Fluor® 488 (1:200) (A-21202, Invitrogen). Scale bar indicates 20 μm. The cell imaging was performed on a Zeiss LSM 510 Meta Confocal Microscope, using a 63x Plan-ApoChromat (NA 1.4) oil objective.

The possibility that A_{2A} adenosine receptors could be involved in the low activation of macrophages was studied and those receptors were probed with a goat polyclonal antibody raised against A_{2A} receptors (1:400) (sc-7504, Santa Cruz

Biotechnology Inc). There is a basal amount of A_{2A} adenosine receptors in macrophages not infected; these are distributed equally in the cell. In contrast, when macrophages were infected with *A. infectoria* conidia, the A_{2A} adenosine receptors seem to gather in clusters (Figure 22).

Mϕ 1h30min

Mϕ +E 1h30min
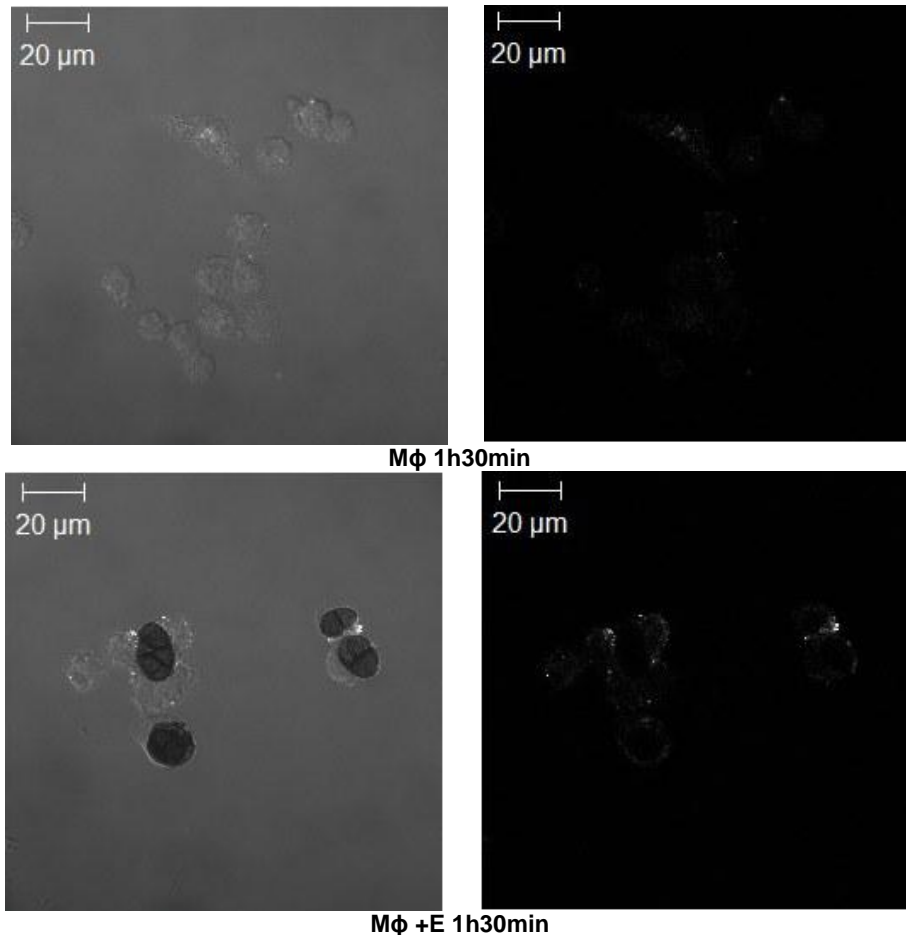
Figure 22. A_{2A} adenosine receptors immunolabeling during *A. infectoria* conidia infection. In macrophages infected by *A. infectoria* conidia (Mϕ+E), the immunostaining is greater in clusters. In contrast, macrophages (Mϕ) present a lower level of immunostaining. Immunocytochemistry was performed using a goat polyclonal antibody raised against A_{2A} receptors (1:400) (sc-7504, Santa Cruz Biotechnology Inc) and anti-goat Alexa Fluor® 647 (1:500) (A-21447, Invitrogen). Scale bar indicates 20 µm. The cell imaging was performed on a Zeiss LSM 510 Meta Confocal Microscope, using a 63x Plan-ApoChromat (NA 1.4) oil objective.

3.5. Relative quantification of A_{2A} adenosine receptor gene (Adora 2a) expression in macrophages during *A. infectoria* conidia infection

Because the A_{2A} adenosine receptors seem to gather in clusters during infection by *A. infectoria* conidia (Figure 22), it was relevant to study if the expression of A_{2A} adenosine receptor gene (Adora 2a) is altered by the presence of the pathogenic agent *A. infectoria* conidia.

The real time RT-PCR (qPCR) showed that in a population of macrophages infected with *A. infectoria* conidia, the expression of the Adora 2a gene did not change, as proved by the relative amounts of specific mRNA (Figure 23). Although some fluctuation on the gene expression was quantified during the time course of infection, it had no significance.
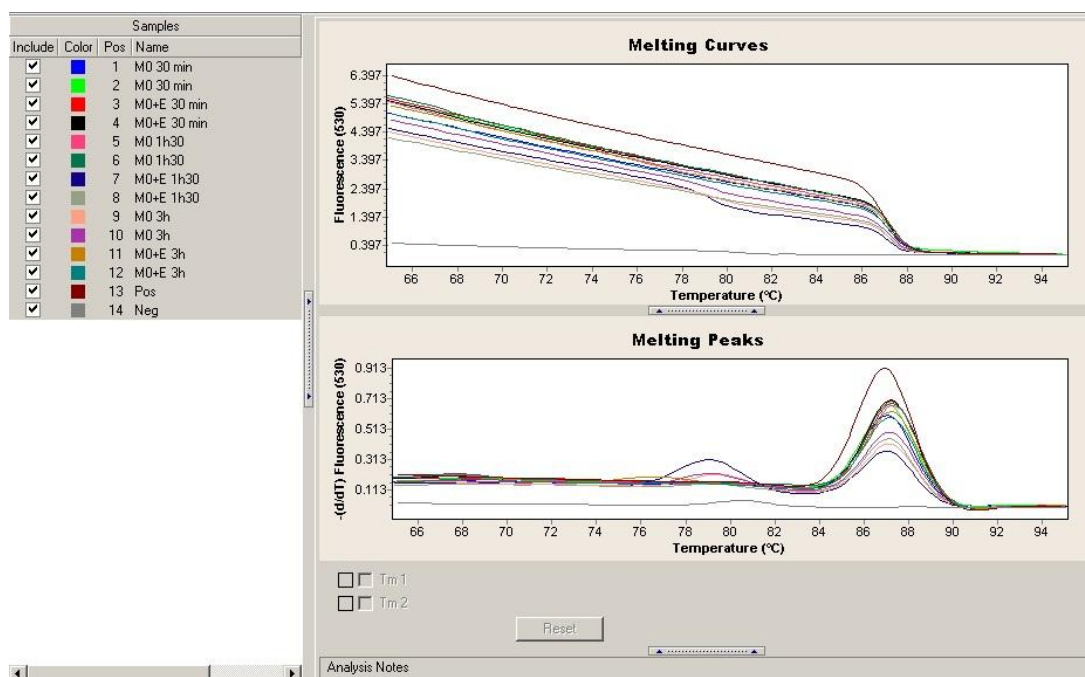
a)
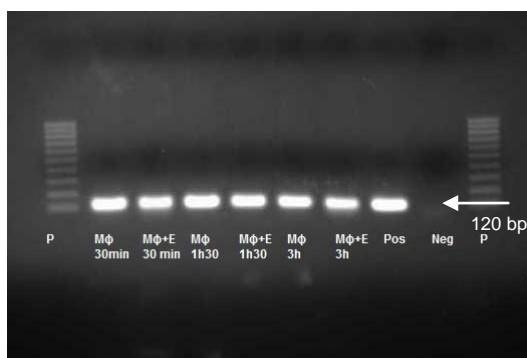
b)
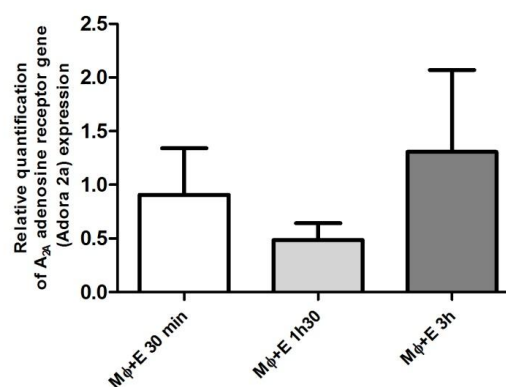
c)

Figure 23. Relative quantification of A_{2A} adenosine receptor gene (Adora 2a) expression in macrophages during *A. infectoria* conidia infection. a) Dissociation curve obtained from the RT-PCR real time products. The relative quantification of the Adora 2a gene was analysed through the dissociation curve obtained from the PCR reaction, which used the SyBR Green fluorophor. The maximum peak of the curve occurs at 87 ºC and corresponds to a single amplicon. The 18S gene was used as reference. The data was analyzed by relative quantification using the $2^{-\Delta\Delta Ct}$ method for each gene using the Ct values (Schmittgen & Livak, 2008). **b)** Profile of the obtained RT-PCR real time products in an agarose gel electrophoresis, showing a single, well-defined band at 120 bp, which corresponds to the amplicon (P: Molecular Ruler 100-1000 pb Bio-Rad[®]; Mφ: macrophages; Mφ+E: macrophages + *A. infectoria* conidia; Pos: Positive control; Neg: Negative control). **c)** Relative quantification of Adora 2a gene expression in *A. infectoria* conidia infection of macrophages in three different time points. The results are presented as mean ± SEM, with n=3.

Results

3.6. Extracellular ATP quantification

As a result of the growing research on ATP as an endogenous danger signal molecule, it seemed pertinent to evaluate if the levels of extracellular ATP would change in response to *A. infectoria* conidia infection. The obtained values of extracellular levels of ATP correspond to it release, but also to its inherent catabolism.

After 30 min of infection, the extracellular concentration of ATP increased in macrophages infected with *A. infectoria* conidia (Figure 24). Even though the levels of extracellular ATP increase slightly after 1h30min of infection and 3 h, the difference is not significant. A supplementary analysis, where variation between the concentration in each time of infection was calculated, further evidencing no significant differences throughout the time of infection (Figure 24, insert).
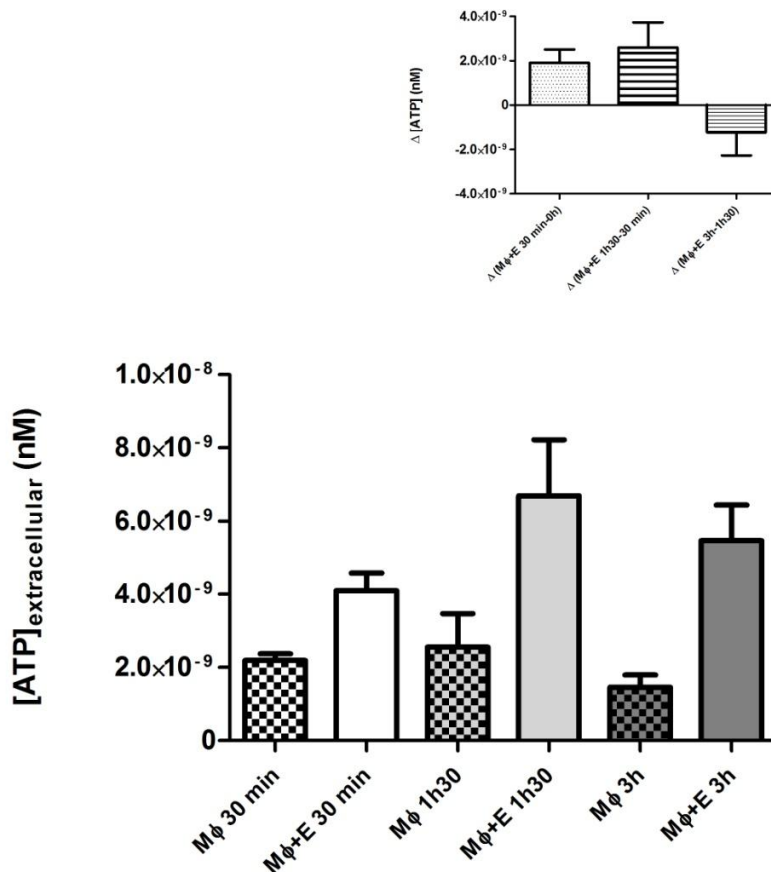
Figure 24. Extracellular ATP quantification. Quantification of extracellular ATP (nM) in macrophages during *A. infectoria* conidia infection. At 30 min of infection the levels of extracellular ATP increased in macrophages infected with *A. infectoria* conidia (Mφ+E). After 1h30min and 3 h of infection the levels of extracellular ATP in infected macrophages stabilize. (**insert**: Variation of extracellular ATP concentration (nM) between times of infection. The submitted values of Δ extracellular ATP concentration concern the variation between the final concentration of ATP and the initial one). No significant differences in the Δ extracellular ATP levels were found. The results are presented as mean ± SEM, with n=3.

Chapter 4
Discussion

4. Discussion

Over the last decades, fungi have been increasingly associated with a broad spectrum of diseases in humans and animals, ranging from acute self-limiting pulmonary manifestations and cutaneous lesions in immunocompetent individuals to inflammatory diseases and life-threatening infections in immunocompromised patients. Because the population of immunocompromised individuals has increased (secondarily to the increased prevalence of chemotherapy, organ transplantation and autoimmune diseases), so has the incidence of fungal diseases (Romani, 2011).

Additionally, some evidences have been progressively contributing for the emergent importance of *A. infectoria* as a human pathogen. In particular, the identification of its importance as one of the most common airborne fungal particles, stimulates the growing research interest on the mechanisms by which this opportunistic pathogen can cause disease (Gergen, 1992; Halonen *et al.*, 1997; Nelson *et al.*, 1999; Arbes *et al.*, 2007; Murai *et al.*, 2012).

The main goal of this research was to characterize the innate immune response of macrophages to *A. infectoria* conidia*. In vitro* experiments employing a mouse macrophage cell line, RAW 264.7, allowed the identification of unique morphological and biochemical features of this critical interaction between a phagocyte and *A. infectoria* conidia. Moreover, this work proved some established assumptions concerning the production of endogenous danger signals in a fungal infection. Also, the hypothesis that A_{2A} adenosine receptors could be involved on the final outcome of a fungal infection was validated in the case of an *A. infectoria* conidia infection.

4.1. Characterization of *A. infectoria* conidia phagocytosis by macrophages

Phagocytes – including macrophages – have several roles in immunity, inflammation and tissue repair. Furthermore, they are the key players in innate immune response to microorganisms and in the initiation of adaptive immune responses. As the term "phagocytes" demonstrates, these professional phagocytic cells are the experts in phagocytosis, the process whereby cells "eat" a wide variety of targets, including microorganisms, dead cells and environmental debris (Underhill & Goodridge, 2012).

Since the major objective of this research work was to characterize the innate immune response to *A. infectoria*, the first step was to show how macrophages behave when challenged with *A. infectoria* conidia.

Live cell video microscopy offers a multiple additional layers of information for analysis. More importantly, this method enables differential analysis of the individual stages of phagocytosis: first, migration of phagocytes to the site where the pathogens

are located; secondly, recognition of PAMPs through PRRs; thirdly, engulfment of the pathogens bound to the phagocyte cell membrane; and fourthly, processing of engulfed cells within maturing phagosomes and digestion of the ingested particle.

As previously described (El-Kirat-Chatel & Dufrêne, 2012), observation of the presence of morphological features that are characteristic of macrophages was achieved: i) well-spread (Figure 7) or round-shaped cells (Figure 9) with a diameter ranging from 10-20 µm; ii) cellular protrusions, with approximately 2 µm of width and 15 µm in length, reflecting lamellipodia, i.e., membrane distortions enriched with a network of actin filaments, which help the cell to migrate (Small *et al.*, 2002; Buccione *et al.*, 2004). The macrophages in Figure 8 displayed lamellipodia extensions as well as pseudopod extensions, suggesting that these cells projected these filaments with the goal of migrating and binding their target (the spores), respectively.

In addition, the observation of cooperativity between macrophages (Figure 9) allied to the detachment of the fungal cell wall and then, the engulfment by a second macrophage; evidence the complexity of inter-macrophage communication during the elimination of the fungal pathogen. This loss of adhesion of the fungal cell wall (when internalization is not achieved within a limited time), followed by the engulfment by a neighbouring macrophage, has been already show for another fungal pathogen, *Candida albicans* (Levitz *et al.*, 2012).

Furthermore, the demonstration that a macrophage containing an internalized spore can still successfully go through division (Figure 10) was achieved. Macrophage division and proliferation plays an important role in the outcome of a fungal infection, mainly as a result of the increase number of phagocytic cells.

Additionally, evidence that appressorium formation can occur both in intra- and extracellularly from the macrophage was demonstrated (Figure 11; Figure 13).

A recent report (Bain *et al.*, 2012), proved that if a fungal cell was internalized, leaving the hyphal tip extracellularly, another macrophage would eventually recognize and engulf it. Nevertheless, in this work it is not clear whether externalized hyphae can be recognized and phagocytosed by a neighbouring macrophage (Figure 12).

The observation of a strange smooth intracellular compartment in an activated macrophage (Figure 14), which is phagocytizing an *A. infectoria* spore, was remarkable. However, if this compartment was localized next to the spore, or if it was just nearby, remains unanswered, probably because the exact location view is beyond the limit of optical microscopy. As to what is this compartment, unfortunately live cell imaging could not elucidate. Nonetheless, its appearance points to a vacuole or a phagosome. The definitive location and characteristics of this compartment should be studied using

electronic microscopy and/or using fluorescent probes for particular intracellular compartments.

Although, the approach of live cell video microscopy, in a minute-by-minute analysis could not fully elucidate the *A. infectoria* conidia phagocytosis by macrophages, this method worked as a good exploratory experiment, since it provided partial and mainly observational insights into the complexity of this interaction.

4.2. Quantification of *A. infectoria* conidia-macrophage interaction

The major bottleneck in the analysis of *A. infectoria* conidia phagocytosis by macrophages is the labelling and counting, since to date this is still carried out manually. Presently, regardless of several efforts, no available labelling is possible for *A. infectoria* conidia. In this work it was demonstrated that wheat germ agglutinin can successfully label these spores, but it also labels macrophages. As a result, determination of internalization, adhesion and appressorium formation percentages must be performed using standard microscopic analysis by a human operator. Overall, the operator bias is not a concern in fungal phagocytic determinations (Mech *et al.*, 2011; Coelho *et al.*, 2012).

Taken together with a statistical analysis, the internalization of *A. infectoria* conidia by macrophages (Figure 15) was, starting at 30 min and through the 6 h of infection, around 55-70 %.

In 2002, Wasylnka and Moore, quantified the percentage of internalized *A. fumigatus* conidia by a murine macrophage cell line J774, evidencing that these cells internalized approximately 90% of the bound conidia (Wasylnka & Moore, 2002). In 2007, Warwas and colleagues also observed a 74% of internalization of *A. fumigatus* conidia in J774 cells (Warwas *et al.*, 2007). The difference between both works can be due to the fact that a different MOI in the phagocytosis assay was used.

Another striking feature of the interaction between *A. infectoria* conidia and macrophages is that at 1h30min of infection, the adhered conidia decrease (Figure 16). Possibly, the adhered spores if not internalized after a limit of time, lose adhesion (whether as a result of the macrophage or the spore), so that another macrophage can engulf them. This is even more obvious in *A. infectoria* conidia because of their larger size (when comparing with *A. fumigatus* conidia), which will consequently decrease the number of internalized spores per macrophage.

Moreover, the observation that macrophages did not significantly delayed germination in phagocytosed conidia (Figure 17; Figure 18) further revealed the lack of effectiveness of macrophages against a germinating spore.

Previous studies in our research group have successfully characterized the viability of *A. infectoria* conidia after ingestion by macrophages. Briefly, the results showed that at 6 h of infection 60% of the conidia were still viable. Also, at this time, macrophage viability was heavily reduced and hyphae formation evident.

4.3. TNF-α release in macrophages during the course of infection with *A. infectoria* conidia

Cytokines are important mediators of the immune system and their production is crucial for determining the outcome of fungal infections. TNF-α is a proinflammatory cytokine necessary for the development of effective innate and adaptive immunity to fungal infections. It stimulates antifungal effector functions of neutrophils and/or macrophages against *C. albicans*, *A. fumigatus* and *Cryptococcus neoformans* (Roilides et al., 1998; Kawakami et al., 1999; Netea et al., 2004; Antachopoulos & Roilides, 2005). The role of TNF-α in the development of protective T_H1 responses was demonstrated in animal models of candidiasis, aspergillosis and cryptococcosis (Bauman *et al.*, 2003).

Examination of the levels of TNF-α (a proinflammatory cytokine) during *A. infectoria* conidia infection of macrophages (Figure 19) revealed a remarkable feature of the pathogenesis of this organism. In contrast, with other fungal infections, there was not an increase in the production of TNF-α in response to *A. infectoria* conidia infection of macrophages. Similar observations were made for the facultative intracellular pathogen *Candida glabrata*, indeed, Seider and colleagues showed that there was no production of the major proinflammatory cytokines (namely, TNF-α) in infected macrophages (Seider *et al.*, 2011).

Most of *A. infectoria* conidia seem to overcome and remain viable after phagocytosis by macrophages, which together with an inefficiency of macrophages to produce and release TNF-α can mean the existence of immune evasion strategies employed by the spores to self-perpetuate in the host cells.

4.4. Immunocytochemistry assay for TLR2, A_{2A} adenosine receptors, N-acetyl-D-glucosamine and sialic acid

Sialic acids are a family of sugars with a shared nine-carbon monosaccharide and are always found as the terminal monosaccharides attached to the glycans on the cell surface (Lin *et al.*, 2010; Varki & Gagneux, 2012).

A number of human fungal pathogens have been found to express sialic acids on their cell surface, for instance, *C. neoformans, C. albicans* and *A. fumigatus* (Rodrigues

et al., 1997; Soares *et al.*, 2000; Wasylnka *et al.*, 2001). The role of sialic acids in fungal pathogenesis is still controversial since it appears to be dependent on the fungal species in study. For example, in *C. neoformans* sialic acids have been implicated in a protective function, because its removal using sialidase, increases the level of phagocytosis (Rodrigues *et al.*, 1997). On the contrary, for *A. fumigatus* the removal of surface sialic acids significantly decreased the conidial uptake by murine macrophage cells J774 (Warwas *et al.*, 2007).

In this work, labeling of N-acetyl-D-glucosamine (monomer of chitin) and sialic acids was accomplished for both *A. infectoria* conidia and macrophages (Figure 20), demonstrating that the presence of these residues could be of great importance for the study of this pathogenic interaction.

TLR2 is a PRR that recognizes phospholipomannan. Several studies have demonstrated that although TLR2 ligation can stimulate proinflammatory cytokine production, this effect is weaker that that mediated by other TLRs. Furthermore, TLR2 ligands fail to induce the T_H1-type IFN-γ, hence promoting conditions that are favourable for a T_H2- or T_{Reg}-type responses (Netea *et al.*, 2008). TLR2 has received renewed attention after the report that demonstrated a synergism between TLR2 and dectin-1.

The hypothesis that infected macrophages would display a different profile in the membrane distribution of this protein turn out invalid (Figure 21). One explanation for this can be that *A. infectoria* conidia do not exhibit TLR2 ligands on their cell walls.

As already addressed previously, adenosine receptors act as negative regulators of immune cells in several models of acute inflammation. Increasing evidence supports the essential role of A_{2A} adenosine receptors in the inflammatory and immune responses (Morello *et al.*, 2009).

A_{2A} adenosine receptors on the cell membrane of *A. infectoria* conidia-infected macrophages were gathered in clusters (Figure 22). On the contrary, in non-infected macrophages an equal distribution throughout the membrane was found.

Seemingly, these results evidence a major difference in what concerns the role of this receptor in the immune response consequent of *A. infectoria* conidia infection. Moreover, exchange of receptors between membrane domains is a critical aspect of cellular sensitivity to extracellular cues (Lajoie *et al.*, 2009). A new concept for interactions between cells of the adaptive immune system and more recently of phagocytes, have emerged in the last years. These intracellular junctions are all highly organized in a reaction environment in which numerous receptors and all surface ligands engage juxtacrine functions (Dustin & Groves, 2012). A key organizing element for

signaling receptors appears to be lipid rafts, which presumably provide more stable, efficient signaling platforms for ligand-engaged immune receptors, thus allowing the activation of cells by fewer and lower affinity ligands (Dykstra *et al.*, 2003; Neugart *et al.*, 2012).

Therefore, A_{2A} adenosine receptors might be recruited to these domains during the course of *A. infectoria* conidia infection of macrophages, in order to potentiate the inherent signaling cascades.

4.5. Adora 2a gene expression in macrophages during *A. infectoria* conidia infection

A_{2A} receptors have taken center stage as the primary anti-inflammatory effectors of extracellular adenosine. This broad, anti-inflammatory effect of A_{2A} adenosine receptor activation is a result of the predominant expression of A_{2A} adenosine receptors on monocytes/macrophages, dendritic cells, mast cells, neutrophils, endothelial cells, eosinophils, epithelial cells, as well as lymphocytes and NK cells. A_{2A} adenosine receptor activation inhibits early and late events occurring during an immune response, which include antigen presentation, costimulation, immune cell trafficking, immune cell proliferation, proinflammatory cytokine production, and cytotoxicity (Haskó *et al.*, 2008).

Moreover, LPS causes a strong induction of A_{2A} mRNA in macrophages and corresponding increases in A_{2A} adenosine receptors density and potency to inhibit macrophage activation (Sullivan *et al.*, 2005).

The obtained results regarding the Adora 2a gene expression in *A. infectoria* conidia-infected macrophages, showed no significant differences (Figure 23). However, and taken together with the lack of TNF-α release during the course of infection, Adora 2a gene expression results further evidence that the spores do not induce a proinflammatory response in macrophages, which in turn does not require the intervention of these receptors, and consequently an overexpression of the Adora 2a gene.

4.6. Extracellular ATP levels during *A. infectoria* conidia infection

Autocrine and paracrine ATP signaling can contribute to cellular responses to pathogens, such as the production and release of inflammatory mediators. In numerous cases, agents that contribute to pathogenicity increase the extent of basal release of ATP. Furthermore, ATP signaling in response to pathogens stimulates apoptosis through activation of $P2X_7$ receptors, perhaps as an attempt to fight infection (Corriden & Insel, 2010).

Since ATP release is considered to be a proinflammatory signal, and its catabolism originates adenosine (which is a strong mediator of anti-inflammatory responses), it seemed important to determine if ATP release by *A. infectoria* conidia-infected macrophages would increase. As Figure 24 showed, an initial increase in the released levels of ATP is noted, but over the time no major differences were found. This means that no proinflammatory response was generated during infection. Again, together with the lack of TNF-α release and no overexpression of the Adora 2a gene expression, ATP release levels during infection demonstrate that *A. infectoria* conidia do not provoke a proinflammatory response by macrophages.

Chapter 5
Final Conclusions
Future Perspectives

5. Final Conclusions and Future Perspectives

The main goal of this work was to study the innate immune response of macrophages to *A. infectoria* conidia. In fact, fungal infections are life-threatening and emergent diseases, mainly because of the increase of the immunocompromised population and of allergic diseases due to airborne fungal spores.

The most important conclusion drawn from the present work is that *A. infectoria* conidia do not trigger a proinflammatory response in macrophages. Even though the complete molecular mechanisms associated with the nonexistence of a proinflammatory response were not identified, some clues were discerned. Firstly, no increased in the production and release of TNF-α was found during the *A. infectoria* conidia infection of macrophages. Secondly, the Adora 2a gene expression did not change with the macrophage infection by conidia. Thirdly, extracellular ATP levels did not increase substantially with *A. infectoria* conidia infection. Taken together, these results point clearly to a lack of inflammation triggering.

In addition, *A. infectoria* conidia recognition by macrophages proved to be independent from TLR2 signaling, while A_{2A} adenosine receptors were found to accumulate in clusters during conidial infection.

Moreover, we conclude that although engulfment of conidia by macrophages was a very fast process; macrophages neither delayed germination in phagocytosed conidia, nor did they stop mitotic division, even while containing internalized conidia.

Nevertheless, it remains to be elucidated if the response of macrophages to spores is similar a hyphae response. During this work it was initiated this task, optimizing the extraction methodologies to obtain cell wall extracts with the final purpose of characterizing the macrophage response to *A. infectoria* hyphae cell wall (Annex 1- Supplementary work).

This research work represents the first approach to the study of *A. infectoria* pathogenesis, in particular the macrophage response to this pathogenic fungus infection. However, much more needs to be uncovered and some of the main questions still unanswered are:

- Does the quantity of A_{2A} adenosine receptors change during *A. infectoria* conidia?

- Are the infected macrophages progressing with a normal cell cycle?
- Have sialic acids a protective role in the phagocytosis of *A. infectoria* conidia by macrophages?
- Why do A_{2A} adenosine receptors form clusters in macrophages that have phagocytosed conidia?
- What is the compartment found in activated macrophages?
- Are ROS being successfully produced in the phagolysosome?
- And, what is the macrophage response to *A. infectoria* hyphae? Is it the same as for conidia?

Chapter 6
Bibliographic References

6. Bibliographic references

Antachopoulos, C. and E. Roilides (2005). "Cytokines and fungal infections." <u>British Journal of Haematology</u> **129**(5): 583-596.

Arbes, S. J., P. J. Gergen, B. Vaughn and D. C. Zeldin (2007). "Asthma Cases Attributable to Atopy: Results from the Third National Health and Nutrition Examination Survey." <u>J Allergy Clin Immunol.</u> **120**(5): 1139-1145.

Arbes, S. J., P. J. Gergen, B. Vaughn and D. C. Zeldin (2007). "Asthma Cases Attributable to Atopy: Results from the Third National Health and Nutrition Examination Survey." <u>J Allergy Clin Immunol.</u> **120**(5): 1139-1145.

Bain, J. M., L. E. Lewis, B. Okai, J. Quinn, N. A. R. Gow and L.-P. Erwig (2012). "Non-lytic expulsion/exocytosis of *Candida albicans* from macrophages." <u>Fungal Genetics and Biology</u> **49**(9): 677-678.

Bauman, S. K., G. B. Huffnagle and J. W. Murphy (2003). "Effects of Tumor Necrosis Factor Alpha on Dendritic Cell Accumulation in Lymph Nodes Draining the Immunization Site and the Impact on the Anticryptococcal Cell-Mediated Immune Response." <u>Infection and Immunity</u> **71**(1): 68-74.

Bianchi, M. E. (2006). "DAMPs, PAMPs and alarmins: all we need to know about danger." <u>Journal of Leukocyte Biology</u> **81**(1): 1-5.

Blander, J. M. and R. Medzhitov (2006). "On regulation of phagosome maturation and antigen presentation." <u>Nature Immunol.</u> **7**: 1029-1035.

Bone, D. B. J., D.-S. Choi, I. R. Coe and J. R. Hammond (2010). "Nucleoside/nucleobase transport and metabolism by microvascular endothelial cells isolated from ENT1 $^{-/-}$ mice." <u>Am J Physiol Heart Circ Physiol</u> **299**: H847-H856.

Brown, G. D. (2011). "Innate Antifungal Immunity: The Key Role of Phagocytes." <u>Annu Rev Immunol.</u> **29**: 1-21.

Buccione, R., J. D. Orth and M. A. McNiven (2004). "Foot and mouth: podosomes, invadopodia and circular dorsal ruffles." <u>Nature Reviews Molecular Cell Biology</u> **5**(8): 647-657.

Bibliographic References

Casadevall, A., J. D. Nosanchuk, P. Williamson and M. L. Rodrigues (2009). "Vesicular transport across the fungal cell wall." Trends in Microbiology **17**(4): 158-162.

Casadevall, A., A. L. Rosas and J. D. Nosanchuk (2000). "Melanin and virulence in *Cryptococcus neoformans*." Current Opinion in Microbiology **3**: 354-358.

Coelho, C., L. Tesfa, J. Zhang, J. Rivera, T. Goncalves and A. Casadevall (2012). "Analysis of Cell Cycle and Replication of Mouse Macrophages after *In Vivo* and *In Vitro Cryptococcus neoformans* Infection Using Laser Scanning Cytometry." Infection and Immunity **80**(4): 1467-1478.

Corriden, R. and P. A. Insel (2010). "Basal Release of ATP: An Autocrine-Paracrine Mechanism for Cell Regulation." Science Signaling **3**(104): 1-25.

Dustin, M. L. and J. T. Groves (2012). "Receptor Signaling Clusters in the Immune Synapse." Annual Review of Biophysics **41**(1): 543-556.

Dykstra, M., A. Cherukuri, H. W. Sohn, S.-J. Tzeng and S. K. Pierce (2003). "Locatization is everything: Lipid Rafts and Immune Cell Signaling." Annual Review of Immunology **21**(1): 457-481.

Eduard, W. (2009). "Fungal spores: A critical review of the toxicological and epidemiological evidence as a basis for occupational exposure limit setting." Critical Reviews in Toxicology **39**(10): 799-864.

El-Kirat-Chatel, S. and Y. F. Dufrêne (2012). "Nanoscale Imaging of *Candida*-Macrophage Interaction Using Correlated Fluorescence-Atomic Force Microscopy." ACSNANO **6**(12): 10792-10799.

Ferrer, C., J. Montero, J. L. Alio, J. L. Abad, J. M. Ruiz-Moreno and F. Colom (2003). "Rapid Molecular Diagnosis of Posttraumatic Keratitis and Endophthalmitis Caused by *Alternaria infectoria*." Journal of Clinical Microbiology **41**(7): 3358-3360.

Flannagan, R. S., V. Jaumouillé and S. Grinstein (2012). "The Cell Biology of Phagocytosis." Annual Review of Pathology: Mechanisms of Disease **7**(1): 61-98.

François, J. M. (2007). "A simple method for quantitative determination of polysaccharides in fungal cell walls." <u>Nature Protocols</u> **1**(6): 2995-3000.

Gantner, B. N., R. M. Simmons, S. J. Canavera, S. Akira and D. M. Underhill (2003). "Collaborative Induction of Inflammatory Responses by Dectin-1 and Toll-like Receptor 2." <u>J. Exp. Med</u> **197**(9): 1107-1117.

Gergen, P. a. T., PC. (1992). "The association of individual allergen reactivity with respiratory disease in a national sample: data from the second National Health and Nutrition Examination Survey, 1976-80 (NHANES II)." <u>J Allergy Clin Immunol.</u> **90**(4): 579-588.

Gomez, B. L. and A. J. Hamilton (2002). "Melanins in fungal pathogens." <u>Journal of Medical Mycology</u> **51**: 189-191.

Guarro, F. J. P. a. J. (2008). "*Alternaria* infections laboratory diagnosis and relevant clinical features." <u>Clin Microbiol Infect</u> **14**: 734-746.

Halonen, M., D. A. Stern, A. L. Wright, L. M. Taussig and F. D. Martinez (1997). "Alternaria as a major allergen for asthma in children raised in a desert environment." <u>Am. J. Respir. Crit. Care Med.</u> **155**(4): 1356-1361.

Haskó, G., J. Linden, B. Cronstein and P. Pacher (2008). "Adenosine receptors: therapeutic aspects for inflammatory and immune diseases." <u>Nature Reviews Drug Discovery</u> **7**(9): 759-770.

Hipolito, E., E. Faria, A. F. Alves, G. S. Hoog, J. Anjos, T. Gonçalves, P. V. Morais and H. Estevão (2008). "*Alternaria infectoria* brain abscess in a child with chronic granulomatous disease." <u>European Journal of Clinical Microbiology & Infectious Diseases</u> **28**(4): 377-380.

Hwang, C.-S., M. A. Flaishman and P. E. Kolattukudy (1995). "Cloning of a Gene Expressed during Appressorium Formation by *Colletotrichum gloeosporioides* and a Marked Decrease in Virulence by Disruption of This Gene." <u>The Plant Cell.</u> **7**: 183-193.

Jacobson, E. S. (2000). "Pathogenic roles for fungal melanins." <u>Clinical Microbiology Reviews</u> **13:** 708-717.

Bibliographic References

Kawakami, K., M. H. Qureshi, Y. Koguchi, T. Zhang, H. Okamura, M. Kurimoto and A. Saito (1999). "Role of TNF-a in The Induction Of Fungicidal Activity of Mouse Peritoneal Exudate Cells Against *Cryptococcus neoformans* by IL-12 and IL-18." Cellular Immunology **193**: 9-16.

Kindt, T. J., R. A. Goldsby and B. A. Osborne (2007). Kuby Immunology. New York, Sara Tenney.

Lajoie, P., J. G. Goetz, J. W. Dennis and I. R. Nabi (2009). "Lattices, rafts, and scaffolds: domain regulation of receptor signaling at the plasma membrane." The Journal of Cell Biology **185**(3): 381-385.

Larone, D. H. (2002). Medically important fungi: a guide to identification. Washington, D.C.

Latgé, J.-P. (2007). "The cell wall: a carbohydrate armour for the fungal cell." Molecular Microbiology **66**(2): 279-290.

Latgé, J.-P. (2010). "Tasting the fungal cell wall." Cellular Microbiology **12**(7): 863-872.

Levitz, S. M. (2010). "Innate Recognition of Fungal Cell Walls." PLoS Pathogens **6**(4): e1000758.

Levitz, S. M., L. E. Lewis, J. M. Bain, C. Lowes, C. Gillespie, F. M. Rudkin, N. A. R. Gow and L.-P. Erwig (2012). "Stage Specific Assessment of *Candida albicans* Phagocytosis by Macrophages Identifies Cell Wall Composition and Morphogenesis as Key Determinants." PLoS Pathogens **8**(3): e1002578.

Lin, J. S., J. H. Huang, L. Y. Hung, S. Y. Wu and B. A. Wu-Hsieh (2010). "Distinct roles of complement receptor 3, Dectin-1, and sialic acids in murine macrophage interaction with *Histoplasma* yeast." Journal of Leukocyte Biology **88**(1): 95-106.

Marques, J. M., R. J. Rodrigues, A. C. d. Magalhães-Sant'Ana and T. Gonçalves (2006). "*Saccharomyces cerevisiae* Hog1 Protein Phosphorylation upon Exposure to Bacterial Endotoxin." Journal of Biological Chemistry **281**(34): 24687-24694.

Mech, F., A. Thywißen, R. Guthke, A. A. Brakhage and M. T. Figge (2011). "Automated Image Analysis of the Host-Pathogen Interaction between Phagocytes and *Aspergillus fumigatus*." PLoS ONE **6**(5): e19591.

Milne, G. R. and T. M. Palmer (2011). "Anti-Inflammatory and Immunosuppressive Effects of the A2A Adenosine Receptor." The Scientific World JOURNAL **11**: 320-339.

Morello, S., R. Sorrentino and A. Pinto (2009). "Adenosine A2a receptor agonists as regulators of inflammation: pharmacology and therapeutic opportunities." Journal of Receptor, Ligand and Channel Research **2**: 11-17.

Murai, H., H. Qi, B. Choudhury, J. Wild, N. Dharajiya, S. Vaidya, A. Kalita, A. Bacsi, D. Corry, A. Kurosky, A. Brasier, I. Boldogh and S. Sur (2012). "*Alternaria*-Induced Realease of IL-18 from Damaged Airway Epithelial Cells: An NF-κB Dependent Mechanism of Th2 Differentiation?" PloS ONE **7**(2): e30280.

Nelson, H. S., S. J. Szefler, J. Jacobs, Karen Huss, G. Shapiro and A. L. Sternberg (1999). "The relationships among environmental allergen sensitization, allergen exposure, pulmonary function, and bronchial hyperresponsiveness in the Childhood Asthma Management Program." J Allergy Clin Immunol. **104**(4): 775-785.

Netea, M. G., G. D. Brown, B. J. Kullberg and N. A. R. Gow (2008). "An integrated model of the recognition of *Candida albicans* by the innate immune system." Nature Reviews Microbiology **6**(1): 67-78.

Netea, M. G., B.-J. Kullberg and J. W. M. V. d. Meer (2004). "Proinflammatory Cytokines in the Treatment of Bacterial and Fungal Infections." Biodrugs **18**(1): 9-22.

Neugart, F., D. Widera, B. Kaltschmidt, C. Kaltschmidt and M. Heilemann (2012). "TNF Receptor Membrane Dynamics Studied with Fluorescence Microscopy and Spectroscopy." Springer Ser Fluoresc **13**: 439-455.

Pihet, M., P. Vandeputte, G. Tronchin, G. Renier, P. Saulnier, S. Georgeault, R. Mallet, D. Chabasse, F. Symoens and J.-P. Bouchara (2009). "Melanin is an essential component for the integrity of the cell wall of *Aspergillus fumigatus* conidia." BMC Microbiology **9**(1): 1-11.

Bibliographic References

Pluddemann, A., S. Mukhopadhyay and S. Gordon (2011). "Innate Immunity to Intracellular Pathogens: Macrophage Receptors and Responses to Microbial Entry." Immunological Reviews **240**: 11-24.

Ramakers, B. P., N. P. Riksen, J. G. van der Hoeven, P. Smits and P. Pickkers (2011). "Modulation of Innate Immunity by Adenosine Receptor Stimulation." Shock **36**(3): 208-215.

Rodrigues, M. L., S. Rozental, J. N. Couceiro, J. Angluster, C. S. Alviano and L. R. Travassos (1997). "Identification of N-Acetylneuraminic Acid and Its 9-O-Acetylated Derivative on the Cell Surface of *Cryptococcus neoformans*: Influence on Fungal Phagocytosis." Infection and Immunity **65**(12): 4937-4942.

Roilides, E., A. D. Dou-Georgiadou, T. Sein, I. Kadiltsoglou and T. J. Walsh (1998). "Tumor Necrosis Factor Alpha Enhances Antifungal Activities of Polymorphonuclear and Mononuclear Phagocytes against *Aspergillus fumigatus.*" Infection and Immunity **66**(12): 5999-6003.

Romani, L. (2004). "Immunity to fungal infections." Nature Reviews Immunology **4**(1): 11-24.

Romani, L. (2011). "Immunity to fungal infections." Nature Reviews Immunology **11**(4): 275-288.

Romani, L. and P. Puccetti (2007). "Controlling pathogenic inflammation to fungi." Expert Rev. Anti Infect.Ther. **5**(6): 1007-1017.

Schmittgen, T. D. and K. J. Livak (2008). "Analyzing real-time PCR data by the comparative CT method." Nature Protocols **3**(6): 1101-1108.

Seider, K., S. Brunke, L. Schild, N. Jablonowski, D. Wilson, O. Majer, D. Barz, A. Haas, K. Kuchler, M. Schaller and B. Hube (2011). "The Facultative Intracellular Pathogen *Candida glabrata* Subverts Macrophage Cytokine Production and Phagolysosome Maturation." The Journal of Immunology **187**(6): 3072-3086.

Sitkovsky, M. V. and A. Ohta (2005). "The 'danger' sensors that STOP the immune response: the A2 adenosine receptors?" Trends in Immunology **26**(6): 299-304.

Small, V., T. Stradal, E. Vignal and K. Rottner (2002). "The lamellipodium: where motility begins." <u>Trends in Cell Biology</u> **12**(3): 112-120.

Soares, R. M. A., R. M. d. A. Soares, D. S. Alviano, J. Angluster, C. S. Alviano and L. R. Travassos (2000). "Identication of sialic acids on the cell surface of *Candida albicans*." <u>Biochimica et Biophysica Acta</u> **1474**: 262-268.

Sullivan, Gail W., Lauren J. Murphree, Melissa A. Marshall and J. Linden (2005). "Lipopolysaccharide rapidly modifies adenosine receptor transcripts in murine and human macrophages: role of NF-κB in A2A adenosine receptor induction." <u>Biochemical Journal</u> **391**(3): 575-580.

Thrane, B. A. a. U. (1996). "Differentiation of *Alternaria infectoria* and *Alternaria alternata* based on morphology, metabolite profiles, and cultural characteristics." <u>Can. J. Microbiol</u> **42**: 685-689.

Underhill, D. M. and H. S. Goodridge (2012). "Information processing during phagocytosis." <u>Nature Reviews Immunology</u> **12**(7): 492-502.

van de Veerdonk, F. L., B. J. Kullberg, J. W. M. van der Meer, N. A. R. Gow and M. G. Netea (2008). "Host–microbe interactions: innate pattern recognition of fungal pathogens." <u>Current Opinion in Microbiology</u> **11**(4): 305-312.

Varki, A. and P. Gagneux (2012). "Multifarious roles of sialic acids in immunity." <u>Annals of the New York Academy of Sciences</u> **1253**(1): 16-36.

Warwas, M. L., J. N. Watson, A. J. Bennet and M. M. Moore (2007). "Structure and role of sialic acids on the surface of *Aspergillus fumigatus* conidiospores." <u>Glycobiology</u> **17**(4): 401-410.

Wasylnka, J. A. and M. M. Moore (2002). "Uptake of *Aspergillus fumigatus* Conidia by Phagocytic and Nonphagocytic Cells In Vitro: Quantitation Using Strains Expressing Green Fluorescent Protein." <u>Infection and Immunity</u> **70**(6): 3156-3163.

Wasylnka, J. A., M. I. Simmer and M. M. Moore (2001). "Differences in sialic acid density in pathogenic and non-pathogenic Aspergillus species." <u>Microbiology</u> **147**: 869-877.

Bibliographic References

Willart, M. A. M. and B. N. Lambrecht (2009). "The danger within: endogenous danger signals, atopy and asthma." Clinical & Experimental Allergy **39**(1): 12-19.

Zhang, X. and D. M. Mosser (2008). "Macrophage activation by endogenous danger signals." The Journal of Pathology **214**(2): 161-178.

Annexes

Annex 1

Supplementary work

Task: Characterization of the innate immune response to *A. infectoria* hyphae

Aim: Characterization of the innate immune response of macrophages to *A. infectoria* hyphae cell wall by macrophages.

Materials and methods

Fungal Culture: Mycellia were also grown in liquid Yeast Malt Extract (YME) medium with 4 % yeast extract (A1202-HA, Panreac-Cultimed) (w/v), 10% malt extract (8266, BD) (w/v) and 10% glucose (G8270, Sigma-Aldrich) (w/v) and sterilized by autoclaving (121ºC, 1.2 atm for 20 minutes).

Fungal Growth Conditions: The growth of *A. infectoria* mycelia in liquid YME medium was carried out in sterile erlenmeyer's in a volume ratio of 0.4:1, to allow aeration of the culture. The growth was performed at 30ºC with a constant orbital shaking of 120 rpm, in an orbital shaker (Infors Ag CH-4103 Bottmingen).

A. infectoria **hyphae cell wall isolation:** A*. infectoria* mycelia was grown as described previuosly, lyophilized and conserved at -20ºC. Firstly, *A. infectoria* mycelia cell wall was ground in liquid nitrogen until a powder form was achieved. The mycelia powder obtained was then transferred to 2 mL eppendorfs with 10 mM Tris-HCl pH 8.0, 1 mM EDTA (TE), and centrifuged at 1000g for 1 minute. The supernatant was discarded, while the pellet was resuspended in TE plus a protease inhibitor cocktail (P8215, Sigma-Aldrich) and transferred to 1.5 mL eppendorfs, each containing 1g of acid-washed beads (425-600 µm) (G8772, Sigma-Aldrich). Secondly, cell disruption using Magna Lyser® (Roche) was carried out, by applying four cycles of 4,800 rpm for 20 seconds (with 30 seconds intervals on ice between cell disruption cycles). Thirdly, a centrifugation at 1,000g for 1 minute was performed, and the supernatant was collected. At the same time, 1 mL of TE plus protease inhibitor cocktail was added to the previously 1.5 mL eppendorfs (containing acid-washed beads and pellet), and a new round of cell disruption was accomplished. Then, a centrifugation at 1,000g for 1 minute was performed, and the supernatant was collect to the same falcon as the first one. Again, 1 mL of TE plus protease inhibitor cocktail was added to the eppendorf, which was then vortex and centrifuged at 500 g for 1 minute. The obtained supernatant was again collected and this

71

wash step was repeated six more times. Fourthly, the sum of supernatants obtained was centrifuged at 4,800g for 15 minutes, and the pellet was resuspended in 1 mL TE. Lastly, the resuspended pellet was centrifuged at 3,000g for 5 minutes, and the supernatant was collected and dried overnight at 100ºC. The isolated cell wall was, in the next day, conserved at -20ºC (François, 2007). Overall, this protocol was adapted from François, 2007.

Zeta potential of isolated cell wall: In order to characterize the isolated cell wall from *A. infectoria* mycelia, zeta potential measurement was carried out, using the Beckman Coulter® Delsa™ Nano C Particle Analyser.

Briefly, a standard control (Otsuka Electronics, Osaka, Japan) was used to calibrate the equipment, while isolated cell wall was resuspended by adding distilled water and processed by ultrasound. Zeta potential measurement of the isolated cell wall was then achieved (Beckman Coulter® Delsa™ Nano C version 2.31/2.03 Software).

Results and Discussion

These particles will be used in future works to compare between macrophages response to conidia and to particles made with cell wall components of hyphae. This will be used as a model of immune response to hyphae, since it is not possible to work with these long structures that are not internalized by macrophages.

Zeta potential (ζP) is the electric potential created between the charged groups associated with the surface of a particle and the suspension medium. It can be used to derive information concerning the particle surface charge.

The zeta potential obtained for *A. infectoria* mycelia cell wall (-19.33 ± 0.59 mV) was found to be lower than in other pathogenic fungi, namely *A. fumigatus* (Pihet *et al.*, 2009). However, Pihet and colleagues measured the zeta potential of the conidial surface and not the mycelia as done in this work.